

# Aerodynamic Performance Optimization Of Wind Turbine Blade By Using High Lifting Device

Razeen Ridhwan, Mohamed Alshaleeh, Arunvinthan S

**Abstract:** In the “Aerodynamic performance of wind turbine blade by using high lifting device” described that different velocity flow of air is passing through the wind turbine blade model and analyze through a numerical simulation that the pressure variation occur at that surface of the model. Before we built wind turbine blade in any strong wind blowing region the aerodynamic flow analysis is must for withstand the strong wind affects. In this chapter, basic nature of winds and types, wind affects through the wind turbine blade, formation of internal pressure and atmospheric boundary layer. This project could be done with the help of so many research papers were taken and followed in the literature review. The main tool we used in the project is CFD, so we gave some introduction about the CFD and how it could be used. Then we compared the results at the different models in different angles having with and without flap in 2D and 3D. We didn't do any practical oriented models just we design the model in Gambit and analyze in the Fluent.

**Keywords:** Aerodynamics, Blade with flaps,  $C_L$  VS  $\alpha$ ,  $C_D$  VS  $\alpha$ ,  $C_P$  VS  $X/C$ , CFD, Flaps, High Lifting devices, Riblets, pressure and velocity distribution over wind turbine blades, Wind Turbine.

## 1. Introduction

Wind turbines, like aircraft propeller blades, turn in the moving air and power an **electric generator** that supplies an electric current. Simply stated, a wind turbine is the opposite of a fan. Instead of using electricity to make wind, like a fan, wind turbines use wind to make electricity. The wind turns the blades, which spin a shaft, which connects to a generator and makes electricity. When you talk about modern wind turbines, you're looking at two primary designs: horizontal-axis and vertical-axis. **Vertical-axis wind turbines (VAWTs)** are pretty rare. The only one currently in commercial production is the Darrieus turbine, which looks kind of like an egg beater. In a VAWT, the shaft is mounted on a vertical axis, perpendicular to the ground. VAWTs are always aligned with the wind, unlike their horizontal-axis counterparts, so there's no adjustment necessary when the wind direction changes; but a VAWT can't start moving all by itself -- it needs a boost from its electrical system to get started. Instead of a tower, it typically uses guy wires for support, so the rotor elevation is lower. Lower elevation means slower wind due to ground interference, so VAWTs are generally less efficient than HAWTs. On the upside, all equipment is at ground level for easy installation and servicing; but that means a larger footprint for the turbine, which is a big negative in farming areas. VAWTs may be used for small-scale turbines and for pumping water in rural areas, but all commercially produced, utility-scale wind turbines are **horizontal-axis wind turbines (HAWTs)**.

As implied by the name, the HAWT shaft is mounted horizontally, parallel to the ground. HAWTs need to constantly align themselves with the wind using a yaw-adjustment mechanism. The yaw system typically consists of electric motors and gearboxes that move the entire rotor left or right in small increments. The turbine's electronic controller reads the position of a wind vane device (either mechanical or electronic) and adjusts the position of the rotor to capture the most wind energy available. HAWTs use a tower to lift the turbine components to an optimum elevation for wind speed (and so the blades can clear the ground) and take up very little ground space since almost all of the components are up to 260 feet (80 meters) in the air.

## PROJECT ORGANIZATION

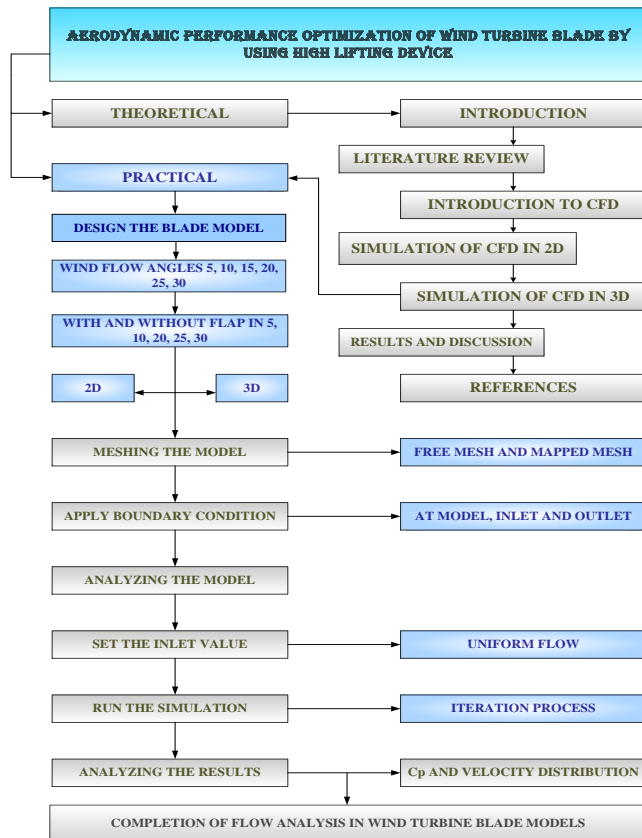
- ❖ Chapter 1 deals with the introduction of nature of wind energy and wind turbine parts and its function, basic blade aerodynamics, influence of atmospheric boundary layer, experimental studies, and methodology and project plan.
- ❖ Chapter 2 deals with the literature survey on the different papers. Influence of equilibrium atmospheric boundary layer and turbulence parameter on wind turbine on riblet model.
- ❖ Chapter 3 deals with the simulation of CFD with introduction, how to works in CFD, methods used to design the model and analyze it, needs to design and create the grid, and grids used in meshing, advantages, limitations and applications of CFD will study in this section.
- ❖ Chapter 4 deals with the influence of high lifting device.
- ❖ Chapter 5 deals with the pressure and velocity distribution of wind turbine with and without flap in 2D models using CFD.
- ❖ Chapter 6 deals with the pressure and velocity distribution of wind turbine with and without flap in 3D models using CFD.
- ❖ Chapter 7 deals with the results and discussion in the pressure distribution occur in the wind turbine blade model it has been shown in the graph. In that graph only we clearly know about that pressure variation occurs in that different point. And how this distribution occurs in that blade model then the compared the

- 
- Razeen Ridhwan U, M.Tech ( Avionics ), Hindustan University, Chennai, Tamil Nadu, India, E-mail :- [rasinridwan@gmail.com](mailto:rasinridwan@gmail.com)
  - Mohamed Alshaleeh.M B.E (Aeronautical Engineering), CAE MODELLER at Ford Technology Services, Chennai, India.
  - Arunvinthan S M.Tech ( Avionics ), asst. professor, JJ ENGG COLLEGE, TRICHY, India.

graph as which it is better we used blade without flap and with flap (in different angle of flap).

- ❖ Chapter 8 deals with the conclusion of this project.
- ❖ Chapter 9 deals with reference that we took review and discuss in the different papers on the different building models. And also took some of the book that we used in the reference.

## METHODOLOGY



## 2. LITERATURE REVIEW

Van Der Hoven and Bechert [30] presented lift characteristics on a 1:4.2 model of Do-228 commuter aircraft model at low speeds; the results show clear evidence of a small increase in lift curve slope (about 1% according to the authors) over the entire a range of  $-51$  to  $+201$  investigated. This slope increase obviously results from reduced boundary layer displacement thickness distributions caused by riblets; essentially riblets lead to a lower viscous decambering effect on the wing. Such a beneficial effect may be expected to be more pronounced on a transonic wing, where the viscous effects play a major role. The sub layers – vortex generators and MEMS technologies which can be used to control flow separation. J.reneaux concluded that Future laminar flow aircraft can, for example, be fitted with wing tip devices and equipped with riblet in the rear part of the wing upper surface. The use of flow control will reduce the system complexity and the structural weight of the aircraft. It is then important to model the effects of sub-layer vortex generators and synthetic jets with the CFD approach. This will allow the gain in performance to be estimated. Gallagher and Thomas explains the drag reduction as coming primarily from a "purely viscous" modification of the sublayer flow, due to the riblet

geometry, that promotes the development of low speed regions within the valley of the grooves in 1984. Kline highlighted the importance of organized deterministic structures in the near-wall turbulence dynamics in 1967. This series of events is usually referred to as the bursting cycle. A. Baron, M. Quadrio and L. Vigevano were discussed about the prediction of turbulent drag reduction by on the boundary layer/ riblets interaction mechanisms. Turbulent drag reduction experienced by ribletted surfaces is the result of both (1) the interaction between riblet peaks and the coherent structures that characterize turbulent near-wall flows, and (2) the laminar sub layer flow modifications caused by the riblet shape, which can balance, under appropriate conditions, the drag penalty due to the increased wetted surface. The latter "viscous" mechanism is investigated by means of an analytical model of the laminar sub layer, which removes geometrical restrictions and allows us to take into account "real" shapes of riblet contours, affected by manufacturing inaccuracies, and to compute even for such cases a parameter, called protrusion height, related to the longitudinal mean flow. By considering real geometries, riblet effectiveness is clearly shown to be related to the difference between the longitudinal and the transversal protrusion heights. A simple method for the prediction of the performances of ribletted surfaces is then devised. The predicted and measured drag reduction data, for different riblet geometries and flow characteristics, are in close agreement with each other. The soundness of the physical interpretation underlying this prediction method is consequently confirmed. Most of them deal with global measurements of effects of riblet on the boundary layer to reduce the drag, but some concerned with the analysis of flow field in the vicinity of and inside the groove. Some preliminary results on the influence of riblet on the structure of a turbulent boundary layer have been discussed by A. Baron and M. Quadrio. Such complex experiments have used particular instrumentation (tunnels with very large turbulent length scales; laser-Doppler anemometry; very small hot wires). A comparison of hot-wire measurements over flat and ribletted walls is described. Details of the experimental apparatus and procedures are given, together with some preliminary results. The test is validated by the calculation of the parameters of the boundary layer, by the comparison of the usual profiles of the stream wise component of the velocity with the available experimental data, and by a conditional analysis of the instantaneous signal. MEAN and RMS profiles for the stream wise component of the velocity evidence, for the riblet plate, an upward shift in law-of-the-wall plots and an overall, small reduction in fluctuation intensities across the boundary layer. Skewness and flatness factors appear to be unchanged. Time series of velocity samples are analyzed by means of power spectra, correlations, and conditional techniques. In particular, the VITA technique, used as an ejection detector, gives results in agreement with previous studies for the flat-plate case, and suggests a moderate increase of the ejection frequency over the riblet surface. Accordingly, the time/space scales of the events appear to be shorter for the riblet-plate flow

## 3. INTRODUCTION OF CFD

The study of fluid motion is called Fluid Dynamics. Commonly, the fluid flow is studied in three ways are Experimental, Theoretical and Numerical (CFD). CFD stands

for Computational Fluid Dynamics and it is defined as the science of predicting fluid flow, heat transfer, mass transfer, chemical reactions, and related phenomena by solving the mathematical equations which govern these processes using a numerical process. However, CFD involves creating a computational mesh to divide up real world continuous fluids into more manageable discrete sections.

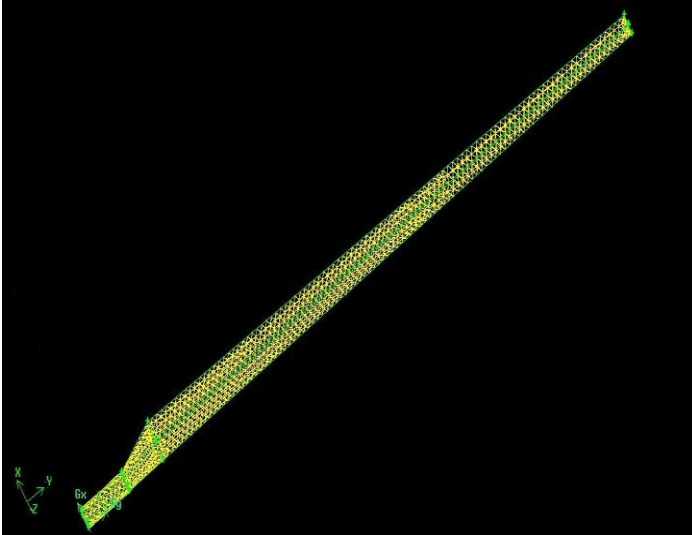


**Figure 3.1 (FLOW OVER A 3D BLADE MODEL)**

The result of CFD analyses is relevant engineering data used in

- Conceptual studies of new design
- Detailed product development
- Troubleshooting
- Redesign

CFD analysis complements testing and experimentation

- Reduces the total effort required in the laboratory.

#### 4. INFLUENCE OF HIGH LIFTING DEVICE

During the design process of wind turbines it is essential to consider many parameters and influencing variables for example wind velocity, rotational speed, engine performance as well as the resulting drag and lift. Especially the last three parameters are dependent on the surrounding flow field. The turbulence level of the wind field, including the high frequency part, influence the transition of laminar to turbulent flows in the boundary layer. As for the wind field only few results of boundary layer investigation exist under realistic conditions: in the field during rotation. As the experimental set-up is rather complex, most research is conducted in wind tunnels. Due to the lack of detailed experimental results for the flow field including the boundary layer, transition and the influence of high frequency turbulence, simplified and empirical methods are used for the performance prediction of wind turbines.

##### 4.1. AERODYNAMIC ANALYSIS AND DESIGN PROGRAM

In order to analyze accurately aerodynamic performance of a blade after stall, the information of stall condition is needed. In general, there are few data after stall, we have to calculate the drag and lift coefficients after stall. Generally, a flap device has been used to decrease the length of takeoff and

landing, but in this study, a flap is used as the high lift device that is devised to design a highly efficient blade. A flap is one of the high lift devices, which is located at the trailing edge of a blade. If the size of a flap is larger than a chord length, the lift to drag ratio become worse, because the amount of lift increase is smaller than that of drag increase. So it is very important to determine the optimum height of a flap for good design. In a three dimensional airfoil of an airplane, tip vortexes are generated due to the pressure difference between the upper and down sides and distribution of circulation surrounding an airfoil decreases. This is the main reason of the loss at a blade tip. A wind turbine also experiences the same phenomena known as blade tip loss.

#### 4.2. TYPICAL VARIATION OF FLAPS

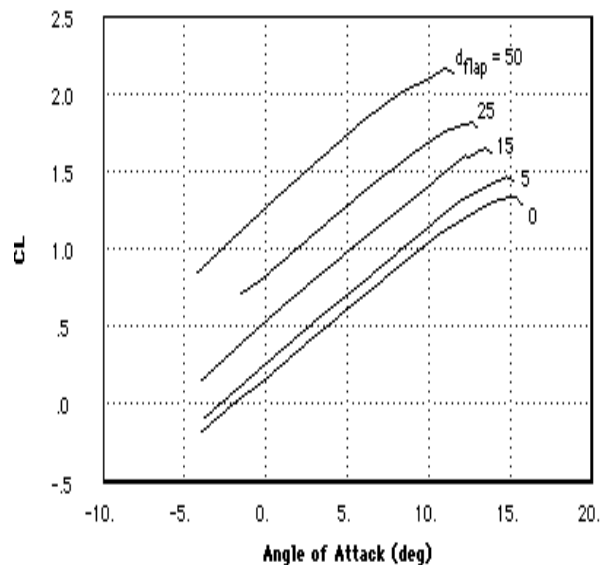


**Figure 4.1. ( $C_L$  vs  $\alpha$ )**

From the above graph we can easily understand how the lift co-efficient ( $C_L$ ) change with the various flaps deflection.

1. Without flap or zero angle deflection of flap the co-efficient of lift is less than 1.5.
2. The flap deflection with  $5^\circ$  co-efficient of lift is near than 1.5 and this value is larger than the co-efficient of lift without flap
3. The flap deflection with  $15^\circ$  co-efficient of lift is more than 1.5 and this value is larger than the co-efficient of lift without flap and also more than co-efficient of lift at  $5^\circ$  deflection

Flap deflection also produces a large change in lift. From fig4.1 the co-efficient of lift is also increased with the increasing of flap deflection.

#### 5. SIMULATION OF WIND TURBINE BLADE IN 2D

Draw the blade model by import the vertex data in the gambit as per steps already discussed in pervious chapter. We need to compare the aerodynamics efficiency of wind turbine blade in different shapes like blade without flap, blade with flap and flap with different angle of deflection of flap. Here we draw the



2D and 3D models. So we draw the 2D models in without flap, flap with  $5^{\circ}$ ,  $10^{\circ}$ ,  $-20^{\circ}$ ,  $20^{\circ}$  &  $25^{\circ}$  deflections.

**5.1. CFD SIMULATION FOR FLAP DIFLECTION (2D)**

- Without flap
- Flap with  $5^{\circ}$  deflection
- Flap with  $10^{\circ}$  deflection
- Flap with  $15^{\circ}$  deflection
- Flap with  $-20^{\circ}$  deflection
- Flap with  $20^{\circ}$  deflection
- Flap with  $25^{\circ}$  deflection

**5.1.1. WITHOUT FLAP**

Import the NACA4415 aerofoil vertex data in GAMBIT and joint the vertex point and draw the aerofoil by jointing the vertex points. After that create the control area at the dimension of 5C from leading edge in the -ve X direction, 20C from trailing edge in +ve X direction and 5C from chord line to top and bottom of chord line. After the facing process subtract the aerofoil face into control area. Now we got a single face.

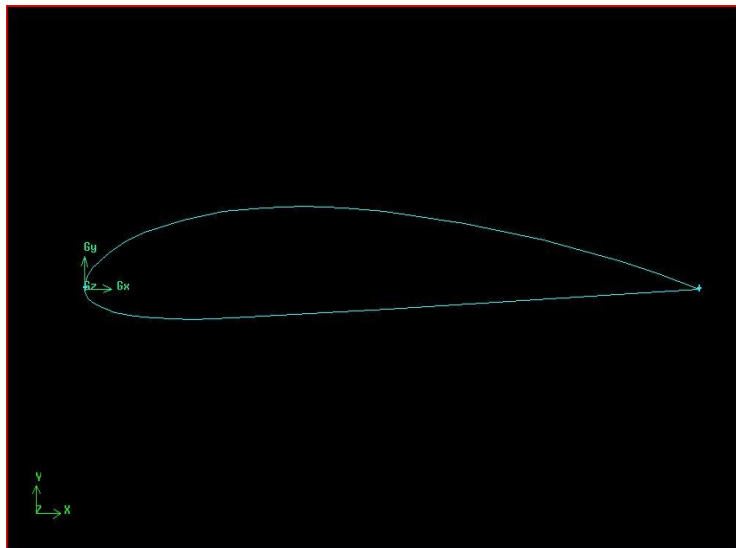


**Figure 5.1**(BLADE WITHOUT FLAP IN 2D)

After the facing process we start meshing the face. First mesh the each line in the model and after finishing the line mesh, mesh the each face mesh. After the meshing process export the model in the “.msh” format. After the modeling the 2D blade we need to analysis the aerodynamic efficiency by using the FLUENT. Read the “.msh” file in the FLUENT and follow the steps which already discussed in chapter3.after finishing the “iterate” process click the contours in display option and see the result of velocity of fluid flow through the model.

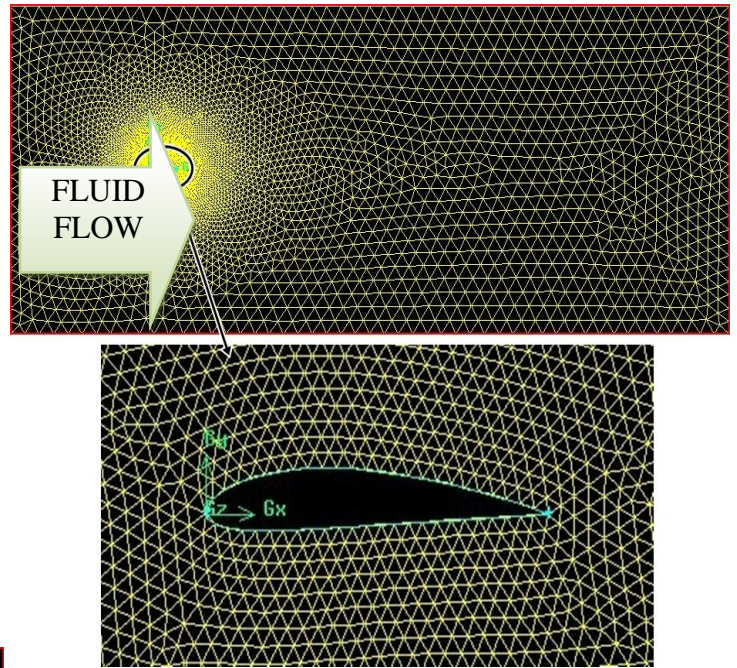


**Figure 5.2** (MESHED WIND TURBINE BLADE WITHOUT FLAP IN 2D)

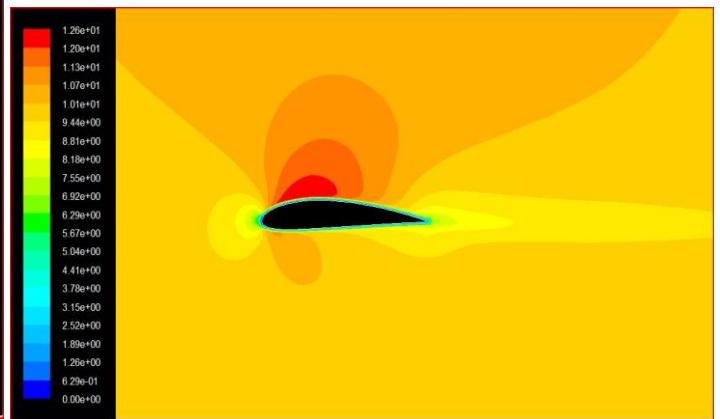


**Figure 5.3** (VELOCITY DISTRIBUTION OF WIND TURBINE BLADE WITHOUT FLAP IN 2D)

We can understand the velocity distribution over the cross-section of 2D model from the above figure. The maximum velocity occurs on the upper surface of the aerofoil. And for pressure distribution click the contours in display option and see the result of pressure of fluid flow through the model.

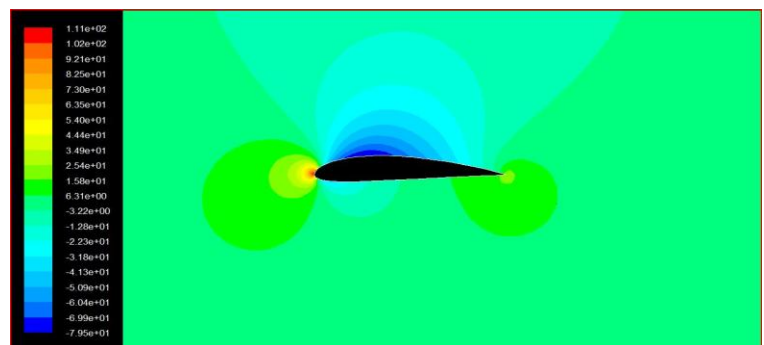


**Figure 5.4 (PRESSURE DISTRIBUTION OF WIND TURBINE BLADE WITHOUT FLAP IN 2D)**

We can understand the pressure distribution over the cross-section of 2D model from the above figure. The maximum pressure occurs on the leading edge of the aerofoil.

**5.1.2. FLAP WITH 5° DEFLECTION**

Import the NACA4415 aerofoil vertex data in GAMBIT and deflect the 20% of chord length from the trailing edge at 5° downward direction. Now joint the vertex point and draw the aerofoil by jointing the vertex points. After that create the control area at the dimension of 5C from leading edge in the -ve X direction, 20C from trailing edge in +ve X direction and 5C from chord line to top and bottom of chord line. After the facing process subtract the aerofoil face into control area. Now we got a single face

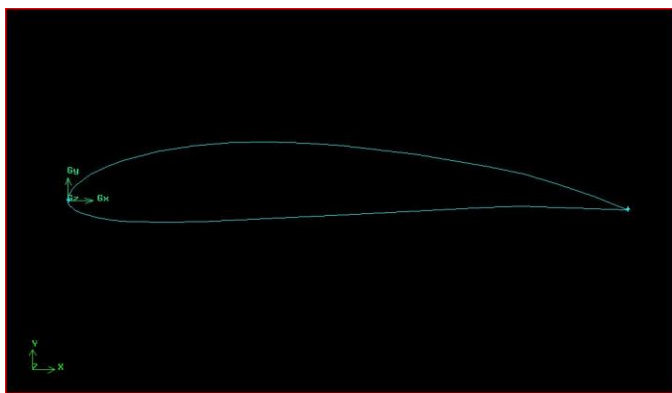


**Figure 5.5 (BLADE WITH FLAP AT 5° DOWNWARD DEFLECTIONS)**

After the facing process we start meshing the face. First mesh the each line in the model and after finishing the line mesh, mesh the each face mesh. After the meshing process export the model in the “.msh” format.

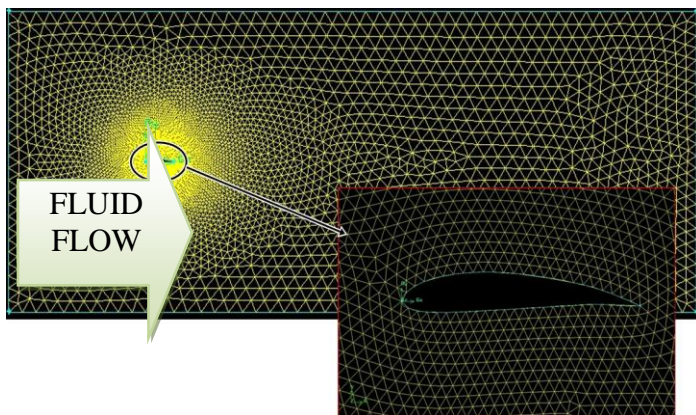


**Figure 5.6 (MESHED WIND TURBINE BLADE WITH FLAP AT 5° DOWNWARD DEFLECTIONS)**

After the modeling the 2D blade we need to analysis the aerodynamic efficiency by using the FLUENT. Read the “.msh” file in the FLUENT and follow the steps which already discussed in chapter3.after finishing the “iterate” process click the contours in display option and see the result of velocity of

fluid flow through the model. We can understand the velocity distribution over the cross-section of 2D model from the below figure5.7. The maximum velocity occurs on the upper surface of the aerofoil. And for pressure distribution click the contours in display option and see the result of pressure of fluid flow through the model. We can understand the pressure distribution over the cross-section of 2D model from the below figure 5.8. The maximum pressure occurs on the leading edge of the aerofoil.

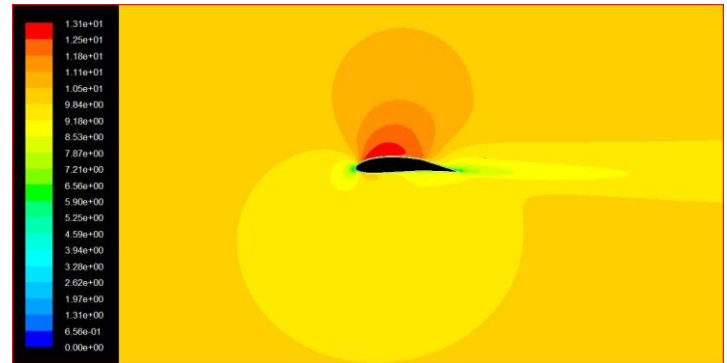


**Figure 5.7 (VELOCITY DISTRIBUTION OF WIND TURBINE BLADE WITH FLAP AT 5° DOWNWARD DEFLECTIONS)**

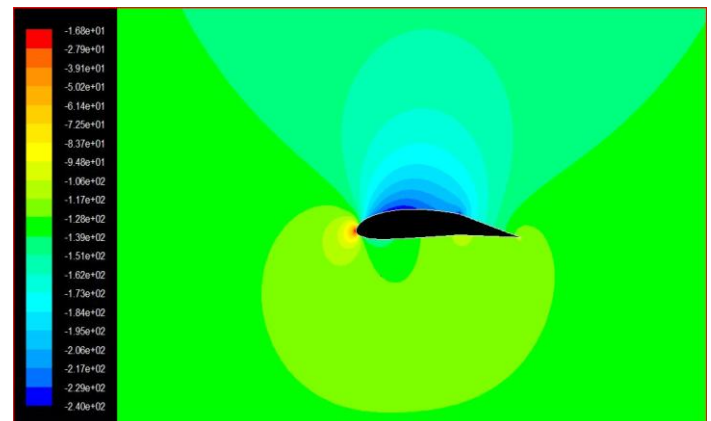


**Figure 5.8 (PRESSURE DISTRIBUTION OF WIND TURBINE BLADE WITH FLAP AT 5° DOWNWARD DEFLECTIONS)**

**5.1.3. FLAP WITH 10° DEFLECTION**

Import the NACA4415 aerofoil vertex data in GAMBIT and deflect the 20% of chord length from the trailing edge at 10° downward direction. Now joint the vertex point and draw the aerofoil by jointing the vertex points. After that create the control area at the dimension of 5C from leading edge in the -ve X direction, 20C from trailing edge in +ve X direction and 5C from chord line to top and bottom of chord line. After the facing process subtract the aerofoil face into control area. Now we got a single face. After the facing process we start meshing the face. First mesh the each line in the model and after finishing the line mesh, mesh the each face mesh. After the meshing process export the model in the “.msh” format.



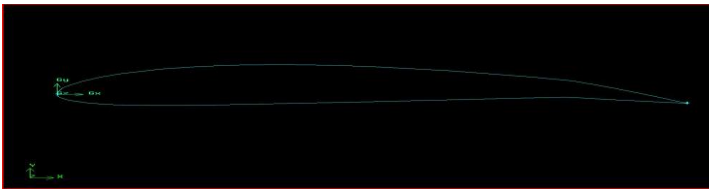


**Figure 5.9** (BLADE WITH FLAP AT 10° DOWNWARD DEFLECTIONS)

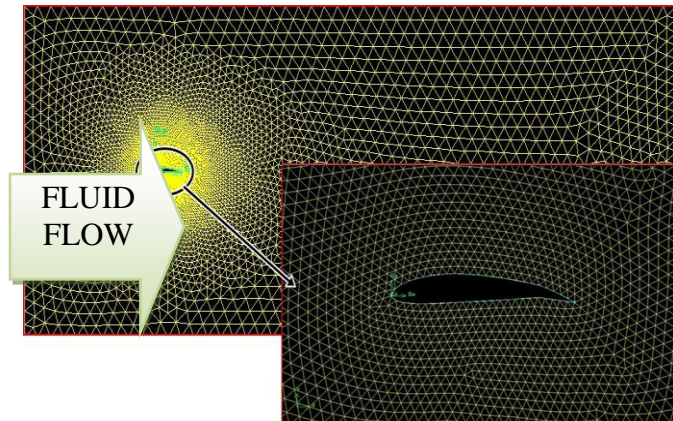


**Figure 5.10** (MESHED BLADE WITH FLAP AT 10° DOWNWARD DEFLECTIONS)

After the modeling the 2D blade we need to analysis the aerodynamic efficiency by using the FLUENT. Read the “.msh” file in the FLUENT and follow the steps which already discussed in chapter3.after finishing the “iterate” process click the contours in display option and see the result of velocity of fluid flow through the model.

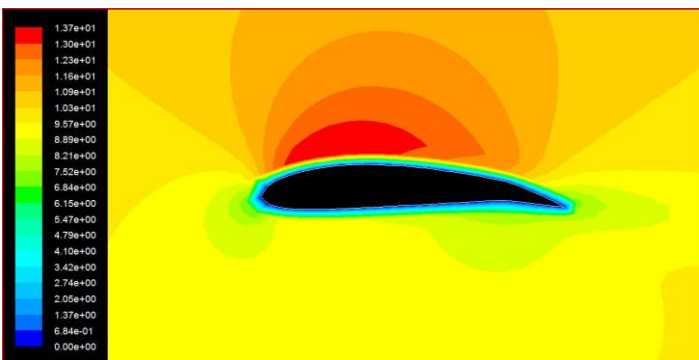


**Figure 5.11** (VELOCITY DISTRIBUTION OF BLADE WITH FLAP AT 10° DOWNWARD DEFLECTIONS)

We can understand the velocity distribution over the cross-section of 2D model from the above figure5.11. The maximum velocity occurs on the upper surface of the aerofoil. And for pressure distribution click the contours in display option and see the result of pressure of fluid flow through the model.

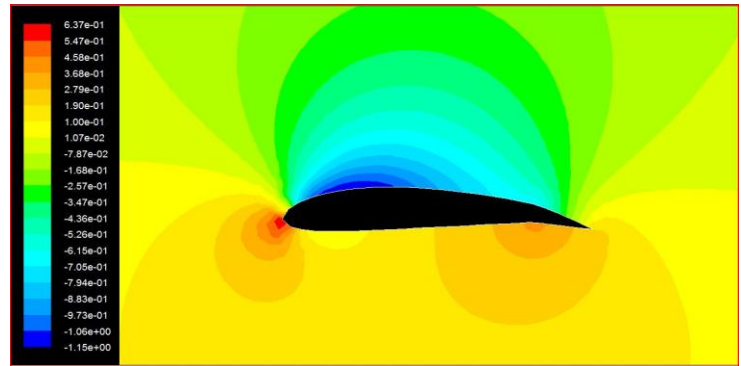


**Figure 5.12** (PRESSURE DISTRIBUTION OF BLADE WITH FLAP AT 10° DOWNWARD DEFLECTIONS)

We can understand the pressure distribution over the cross-section of 2D model from the above figure 5.12. The maximum pressure occurs on the leading edge of the aerofoil. In the upper surface pressure distribution is very low compare then the lower surface.

**5.1.4. FLAP WITH 15° DEFLECTION**

Import the NACA4415 aerofoil vertex data in GAMBIT and deflect the 20% of chord length from the trailing edge at 15° downward direction. Now joint the vertex point and draw the aerofoil by jointing the vertex points. After that create the control area at the dimension of 5C from leading edge in the –ve X direction,20C from trailing edge in +ve X direction and 5C from chord line to top and bottom of chord line. After the facing process subtract the aerofoil face into control area. Now we got a single face.



**Figure 5.13** (BLADE WITH FLAP AT 15° DOWNWARD DEFLECTIONS)

After the facing process we start meshing the face. First mesh the each line in the model and after finishing the line mesh, mesh the each face mesh. After the meshing process export the model in the “.msh” format.

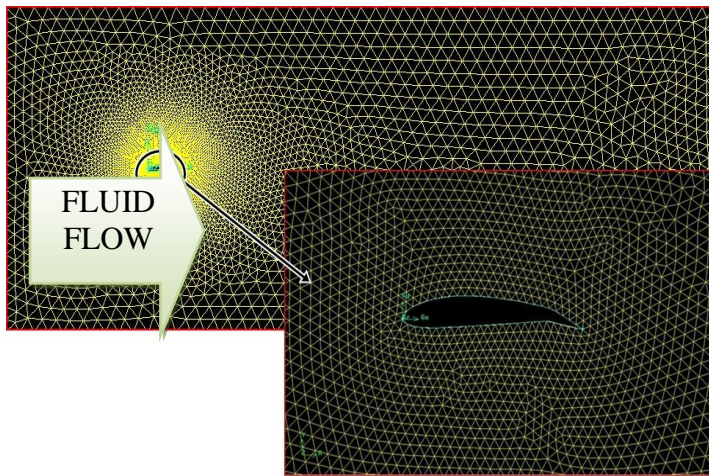


Figure 5.14 (MESHED BLADE WITH FLAP AT 15° DOWNWARD DEFLECTIONS)

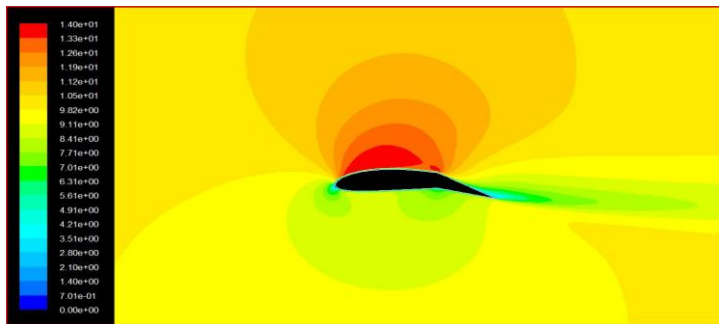


Figure 5.15 (VELOCITY DISTRIBUTION OF BLADE WITH FLAP AT 15° DOWNWARD DEFLECTIONS)

After the modeling the 2D blade we need to analysis the aerodynamic efficiency by using the FLUENT. Read the “.msh” file in the FLUENT and follow the steps which already discussed in chapter3.after finishing the “iterate” process click the contours in display option and see the result of velocity of fluid flow through the model. We can understand the velocity distribution over the cross-section of 2D model from the above figure5.15. The maximum velocity occurs on the upper surface of the aerofoil and also the minimum velocity occurs the leading and trailing edge of the aerofoil. And for pressure distribution click the contours in display option and see the result of pressure of fluid flow through the model. We can understand the pressure distribution over the cross-section of 2D model from the below figure 5.16. The maximum pressure occurs on the leading edge of the aerofoil and also the minimum pressure occurs on the upper surface at point of deflection starts of the aerofoil. . In the upper surface pressure distribution is low compare then lower surface.

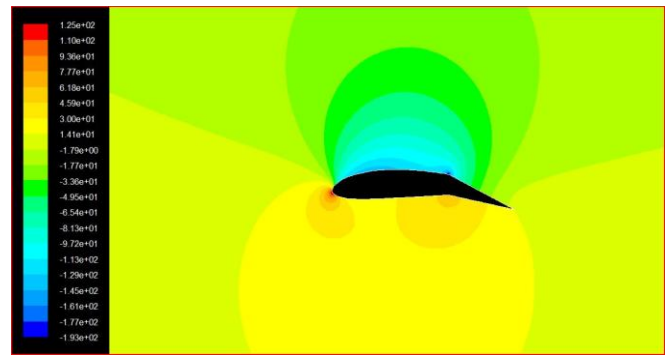


Figure 5.16 (PRESSURE DISTRIBUTION OF BLADE WITH FLAP AT 15° DOWNWARD DEFLECTIONS)

5.1.5. FLAP WITH 20° DEFLECTION

5.1.5.1. FLAP WITH -20° DEFLECTION

Import the NACA4415 aerofoil vertex data in GAMBIT and deflect the 20% of chord length from the trailing edge at 20° upward direction. Now joint the vertex point and draw the aerofoil by jointing the vertex points. After that create the control area at the dimension of 5C from leading edge in the –ve X direction,20C from trailing edge in +ve X direction and 5C from chord line to top and bottom of chord line. After the facing process subtract the aerofoil face into control area. Now we got a single face. After the facing process we start meshing the face. First mesh the each line in the model and after finishing the line mesh, mesh the each face mesh. After the meshing process export the model in the “.msh” format.

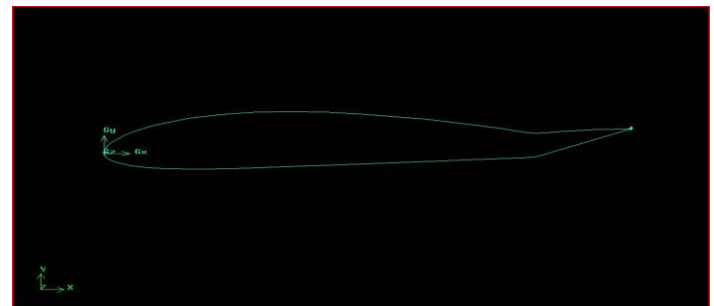


Figure 5.17 (BLADE WITH FLAP AT 20° UPWARD DEFLECTIONS)

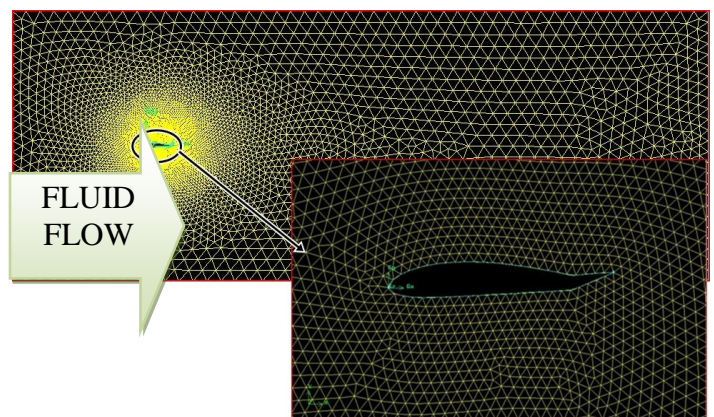
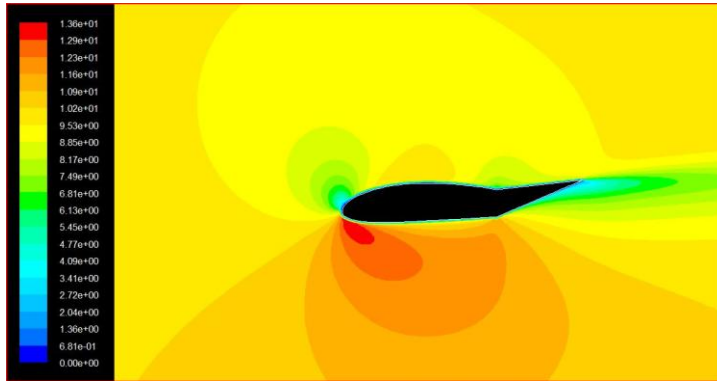


Figure 5.18 (MESHED BLADE WITH FLAP AT 20° UPWARD DEFLECTIONS)



After the modeling the 2D blade we need to analysis the aerodynamic efficiency by using the FLUENT. Read the ".msh" file in the FLUENT and follow the steps which already discussed in chapter3.after finishing the "iterate" process click the contours in display option and see the result of velocity of fluid flow through the model.



**Figure 5.19** (VELOCITY DISTRIBUTION OF BLADE WITH FLAP AT 20° UPWARD DEFLECTIONS)

We can understand the velocity distribution over the cross-section of 2D model from the above figure5.19. The maximum velocity occurs on the lower surface near the leading edge and trailing edge of the aerofoil and also the minimum velocity occurs on the upper surface near the leading edge of the aerofoil. And for pressure distribution click the contours in display option and see the result of pressure of fluid flow through the model.

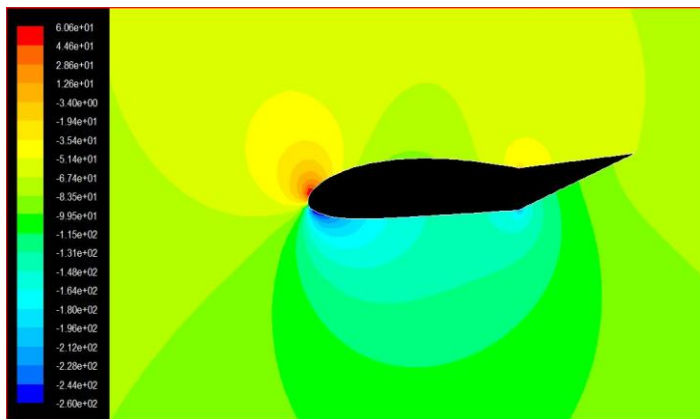


**Figure 5.20** (PRESSURE DISTRIBUTION OF BLADE WITH FLAP AT 20° UPWARD DEFLECTIONS)

We can understand the pressure distribution over the cross-section of 2D model from the above figure 5.20. The maximum pressure occurs on the leading edge of the aerofoil and also the minimum pressure occurs on the lower surface near the leading edge of the aerofoil. In the lower surface the pressure distribution is very low compare then the upper surface.

#### 5.1.5.2. FLAP WITH 20° DEFLECTION

Import the NACA4415 aerofoil vertex data in GAMBIT and deflect the 20% of chord length from the trailing edge at 20° downward direction. Now joint the vertex point and draw the

aerofoil by jointing the vertex points. After that create the control area at the dimension of 5C from leading edge in the –ve X direction, 20C from trailing edge in +ve X direction and 5C from chord line to top and bottom of chord line. After the facing process subtract the aerofoil face into control area. Now we got a single face.

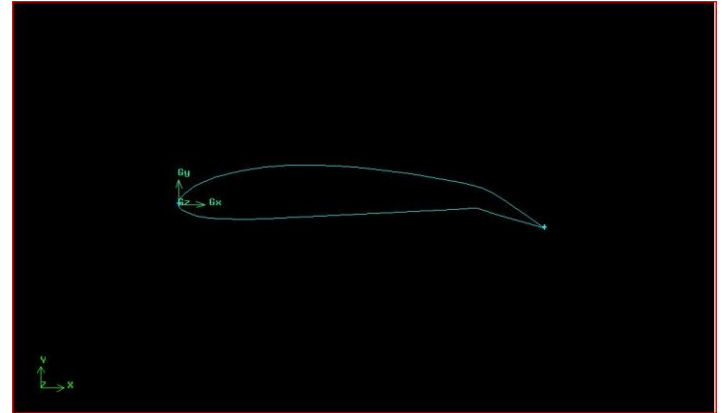


**Figure 5.21** (BLADE WITH FLAP AT 20° DOWNWARD DEFLECTIONS)

After the facing process we start meshing the face. First mesh the each line in the model and after finishing the line mesh, mesh the each face mesh. After the meshing process export the model in the ".msh" format.

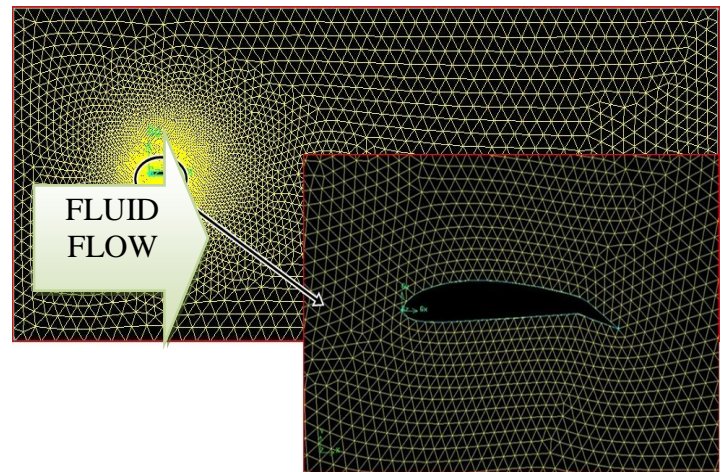


**Figure 5.22** (MESHED BLADE WITH FLAP AT 20° DOWNWARD DEFLECTIONS)

After the modeling the 2D blade we need to analysis the aerodynamic efficiency by using the FLUENT. Read the ".msh" file in the FLUENT and follow the steps which already discussed in chapter3.after finishing the "iterate" process click the contours in display option and see the result of velocity of fluid flow through the model.



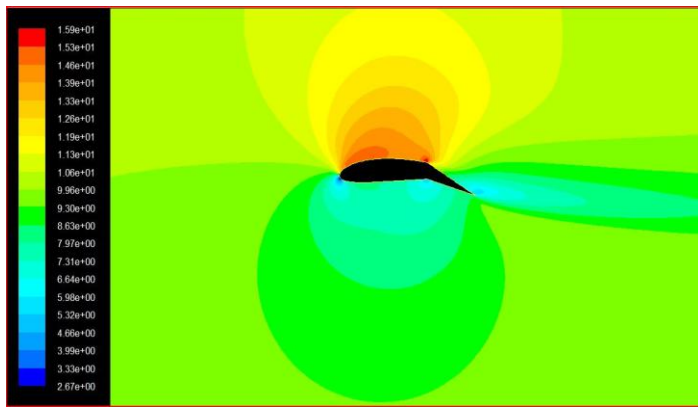


**Figure 5.23 (VELOCITY DISTRIBUTION OF BLADE WITH FLAP AT 20° DOWNWARD DEFLECTIONS)**

We can understand the velocity distribution over the cross-section of 2D model from the above figure 5.23. The maximum velocity occurs on the upper surface at the point which the starting point of the deflection of the aerofoil and also the minimum velocity occurs the leading and trailing edge of the aerofoil. And for pressure distribution click the contours in display option and see the result of pressure of fluid flow through the model.

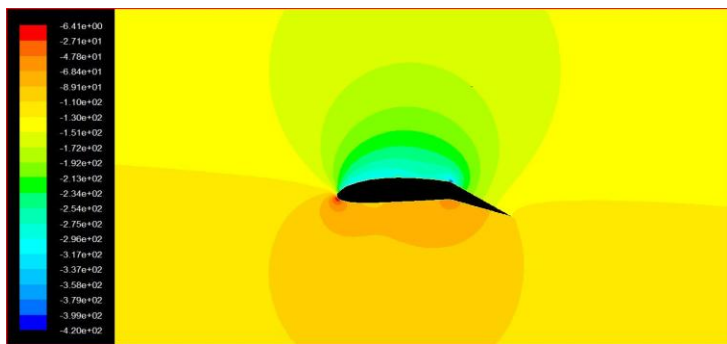


**Figure 5.24 (PRESSURE DISTRIBUTION OF BLADE WITH FLAP AT 20° DOWNWARD DEFLECTIONS)**

We can understand the pressure distribution over the cross-section of 2D model from the above figure 5.24. The maximum pressure occurs on the leading edge of the aerofoil and also the minimum pressure occurs on the upper surface at the point which the starting point of the deflection of the aerofoil. In the upper surface pressure distribution is low compare then lower surface. Here we simulate the wind turbine blade with 20° -ve and +ve deflections. But in the upward (-ve) direction the result was not efficient one that is why we simulate the downward (+ve) in other causes.

**5.1.6. FLAP WITH 25° DOWNWARD DEFLECTION**

Import the NACA4415 aerofoil vertex data in GAMBIT and deflect the 20% of chord length from the trailing edge at 25° downward direction. Now joint the vertex point and draw the aerofoil by jointing the vertex points. After that create the control area at the dimension of 5C from leading edge in the -ve X direction, 20C from trailing edge in +ve X direction and 5C from chord line to top and bottom of chord line. After the facing process subtract the aerofoil face into control area. Now we got a single face.

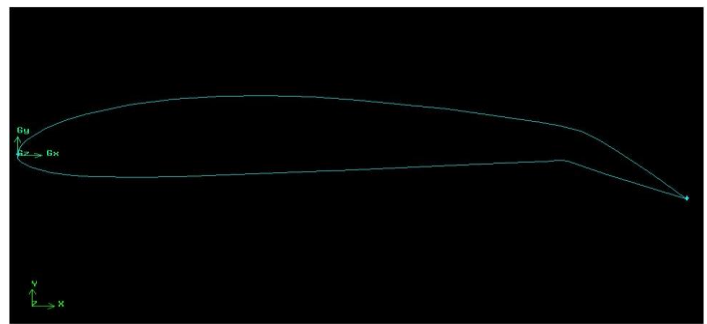


**Figure 5.25 (BLADE WITH FLAP AT 25° DOWNWARD DEFLECTIONS)**

After the facing process we start meshing the face. First mesh the each line in the model and after finishing the line mesh, mesh the each face mesh. After the meshing process export the model in the “.msh” format.

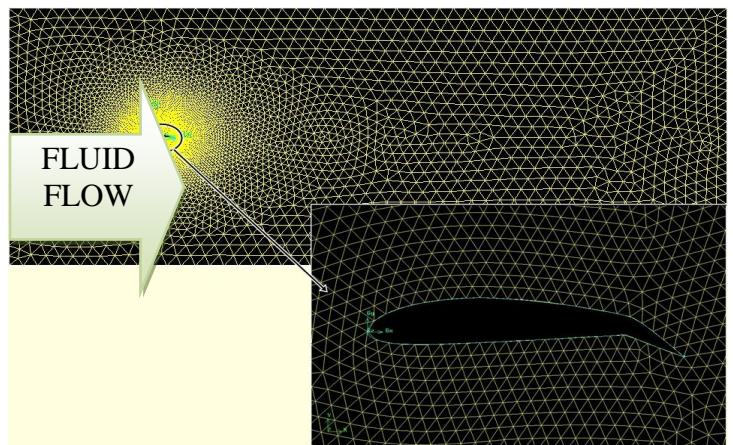


**Figure 5.26 (MESHED BLADE WITH FLAP AT 25° DOWNWARD DEFLECTIONS)**

After the modeling the 2D blade we need to analysis the aerodynamic efficiency by using the FLUENT. Read the “.msh” file in the FLUENT and follow the steps which already discussed in chapter3. after finishing the “iterate” process click the contours in display option and see the result of velocity of fluid flow through the model.

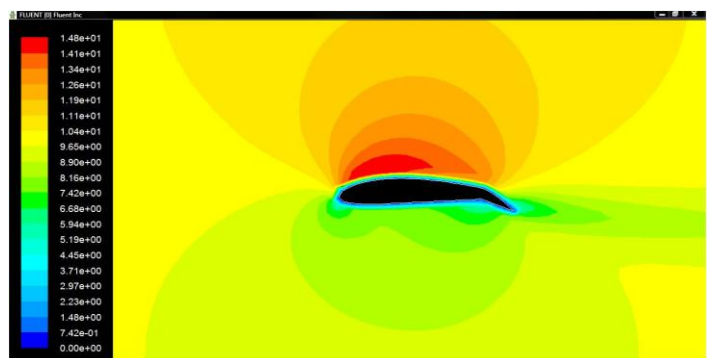


**Figure 5.27 (VELOCITY DISTRIBUTION OF BLADE WITH FLAP AT 25°DOWNWARD DEFLECTIONS)**

We can understand the velocity distribution over the cross-section of 2D model from the above figure 5.27. The maximum

velocity occurs on the upper surface of the aerofoil and also the minimum velocity occurs the leading and trailing edge of the aerofoil. And for pressure distribution click the contours in display option and see the result of pressure of fluid flow through the model. We can understand the pressure distribution over the cross-section of 2D model from the below figure 5.28. The maximum pressure occurs on the leading edge and lower surface at the point of deflection of the aerofoil and also the minimum pressure occurs on the upper surface at the point of the aerofoil. In the upper surface pressure distribution is low compare then lower surface.

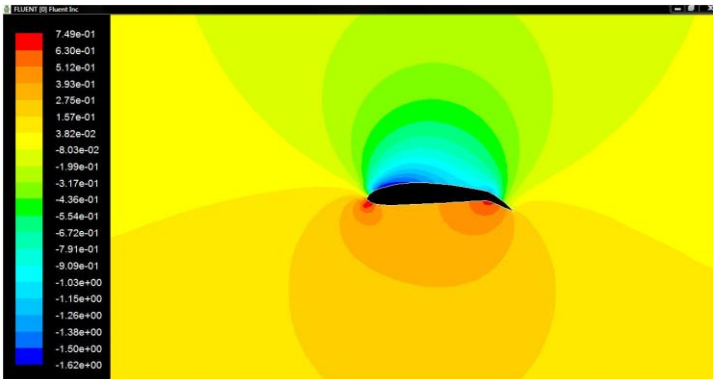


**Figure 5.28 (PRESSURE DISTRIBUTION OF BLADE WITH FLAP AT 25° DOWNWARD DEFLECTIONS)**

From this chapter we can clearly understand the upward deflection of flap is not an efficient one so in 3D we go to discuss about only downward flap deflection in next chapter.

## 6. SIMULATION OF WIND TURBINE BLADE IN 2D

In this chapter we will discuss about the aerodynamic efficiency of wind turbine blade in different shapes like normal blade (without flap) and wind turbine blade with flap with different angle of deflection. From the previous chapter (CFD simulation for flap deflection & its aerodynamic efficiency-2D) we know the upward deflection of flap in wind turbine blade is not efficient. So in this chapter we will discuss only about downward deflection of flap. In this chapter we will discuss the aerodynamic efficiency of wind turbine blade without flap, flap with 5° downward deflection and flap with 10° downward deflection.

### 6.1. CFD SIMULATION FOR FLAP DEFLECTION (3D)

- Without flap
- Flap with 10° downward deflection
- Flap with 20° downward deflection

#### 6.1.1. WITHOUT FLAP

Import the NACA4415 vertex data in different chord length (1.05C at tip of the blade and 2.1C at bottom of blade). The distance between aerofoils was 34.5m. Joint the vertex points and create an aerofoil. Now connect the leading and trailing edges of the aerofoils. This shape looks like an aircraft wing. After the finishing of connection aerofoil we start to draw a cylinder with height 3m and radius 0.5m from the origin (0, 0, and 0). Now we connect the wing to the cylinder (the distance between wing and cylinder is 2.5m). And we get wind turbine blade without flap. After creating the blade model does the

facing process after that does the volume process. Now get a single volume.

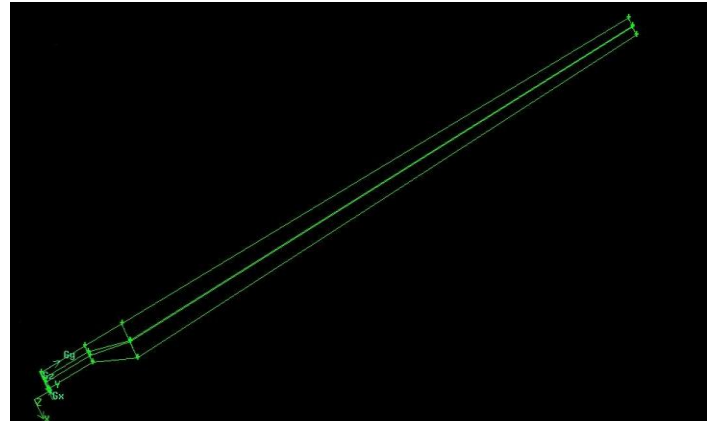


**Figure 6.1 (SINGLE VOLUME BLADE)**

Now we need to create the control volume with the dimension of height 80m (+ve Y-direction), length 80m (60m from centre of cylinder in the direction of +ve X-direction, 20m from centre of cylinder in the -ve X-direction) and depth 40m (20m in +ve Z-direction and 20m in -ve Z-direction). After finishing the creation of control volume subtract the blade volume into control volume. Now we get a single volume.

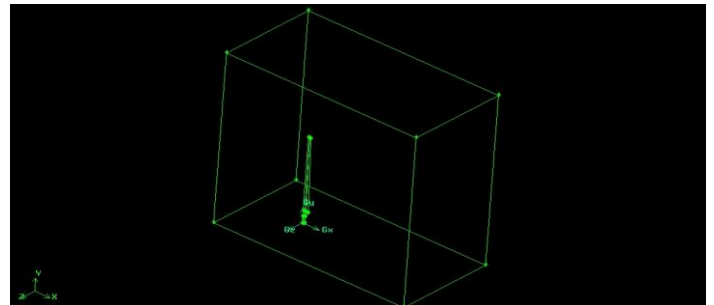


**Figure 6.2 (BLADE WITH CONTROL VOLUME)**

After finishing the volume process we need do the meshing process. First mesh the each line in the model and after finishing the line mesh, mesh the each face mesh. After finishing the face mesh, mesh the full volume by using volume mesh. After the meshing process export the model in the ".msh" format.

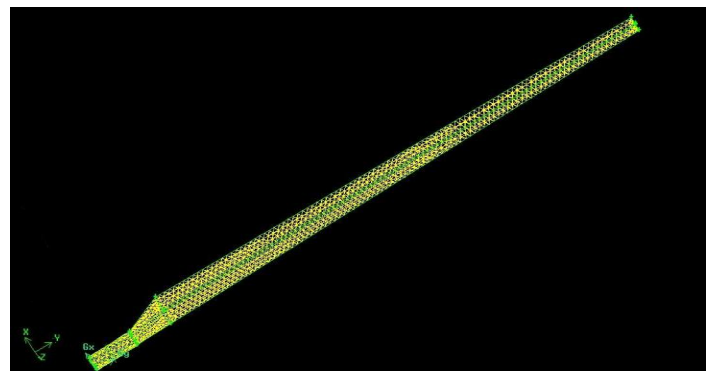


**Figure 6.3.a. (MESHED BLADE)**

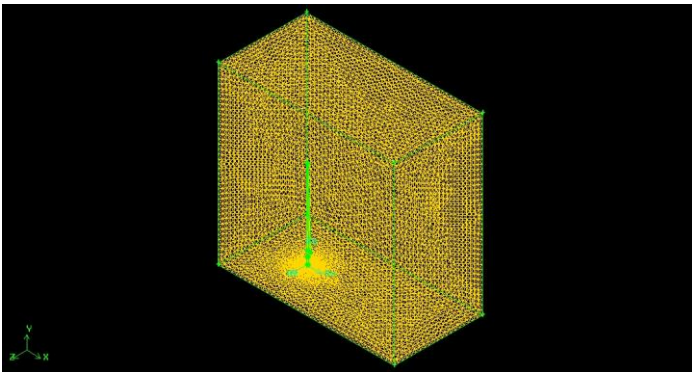


**Figure 6.3.b. (MESHED BLADE WITH CONTROL VOLUME)**

After the modeling the 3D blade we need to analysis the aerodynamic efficiency by using the FLUENT. Read the “.msh” file in the FLUENT and follow the steps which already discussed in chapter3.after finishing the “iterate” process create the Iso-Surface in distance 3m, 4m, 5.5m, 20m and 40m from origin and click the contours in display option and see the result of velocity of fluid flow through the model.

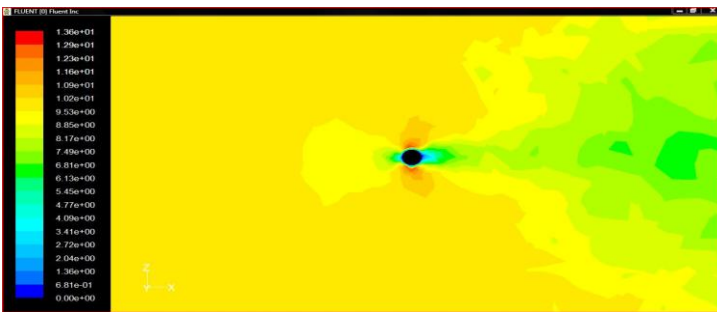


**Figure 6.4 (VELOCITY DISTRIBUTION OF BLADE AT 3M)**

The figure 6.4 is velocity distribution of Iso-surface of blade in 3m from bottom. In the above figure the maximum velocity occurs on upper and lower surface of circle and the minimum velocity occurs in right and left side of the cylinder.

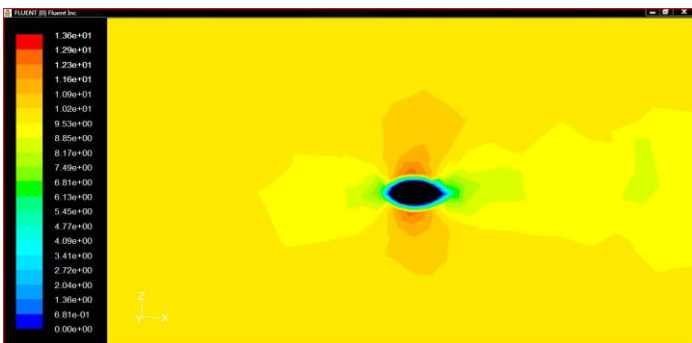


**Figure 6.5 (VELOCITY DISTRIBUTION OF BLADE AT 4M)**

The figure 6.5 is velocity distribution of Iso-surface of blade in 4m from bottom. It is the in between volume of cylinder and wing. In the above figure the maximum velocity occurs on upper and lower surface and the minimum velocity occurs in trailing edge of the cut section.

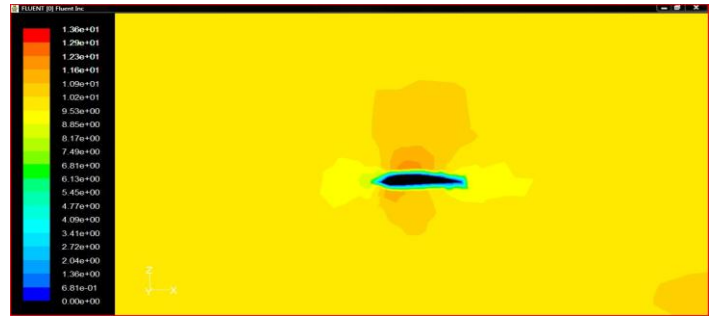


**Figure 6.6 (VELOCITY DISTRIBUTION OF BLADE AT 5.5M)**

The figure 6.6 is the velocity distribution of cut section of blade at 5.5m from the bottom. Here the maximum velocity occurs on the upper surface of the blade and the velocity minimum at leading edge if the blade.

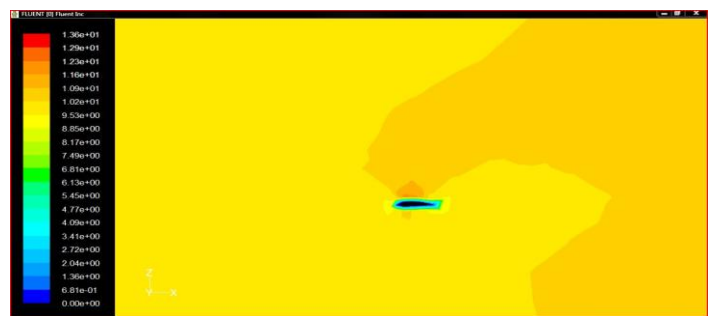


**Figure 6.7 (VELOCITY DISTRIBUTION OF BLADE AT 20M)**

The above figure 6.7 is the velocity distribution of cut section of blade at 20m from the bottom. Here the maximum velocity occurs on the upper surface and other surface in this cut section the velocity is low compare than upper velocity in surface. The below figure 6.8 is the velocity distribution at blade tip. In blade tip normally velocity is more or less same in all faces. And for pressure distribution click the contours in display option and select the Iso-surfaces and see the result of pressure of fluid flow through the model. The below figure 6.9 is pressure distribution of Iso-surface of blade in 3m from bottom. In the above figure the maximum pressure (stagnation pressure) occurs on the leading edge of the cylinder and minimum pressure occurs in upper and lower surface of cylinder.

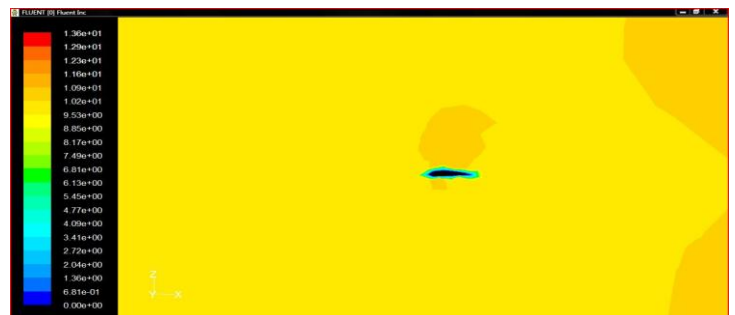


**Figure 6.8 (VELOCITY DISTRIBUTION OF BLADE AT BLADE TIP)**



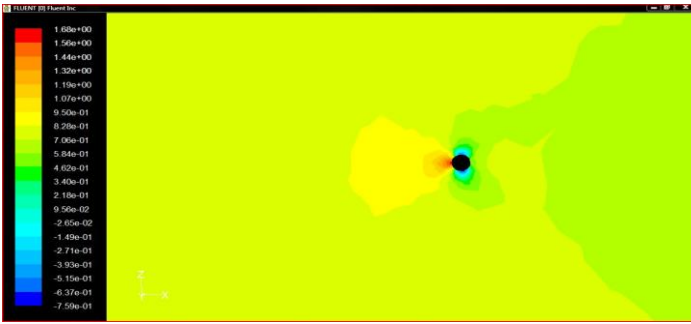


**Figure 6.9 (PRESSURE DISTRIBUTION OF BLADE AT 3M)**

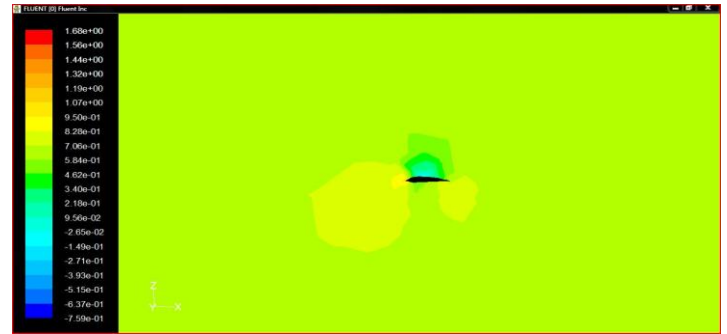


**Figure 6.12 (PRESSURE DISTRIBUTION OF BLADE AT 20M)**

The above figure 6.12 is pressure distribution of Iso-surface of blade in 20m from bottom. In the above figure the maximum pressure (stagnation pressure) occurs on the leading edge of the aerofoil shape and minimum pressure occurs in upper surface of the aerofoil shape.

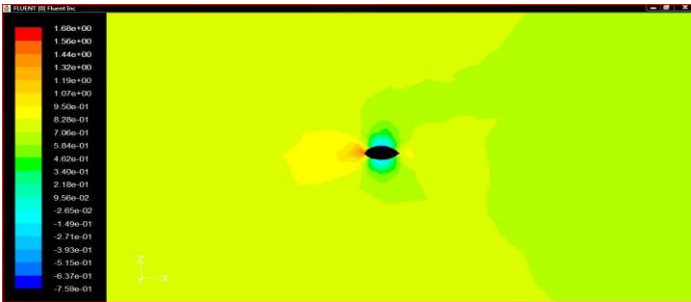


**Figure 6.10 (PRESSURE DISTRIBUTION OF BLADE AT 4M)**

The above figure 6.10 is pressure distribution of Iso-surface of blade in 4m from bottom. In the above figure the maximum pressure (stagnation pressure) occurs on the leading edge of the surface and minimum pressure occurs in upper and lower surface.

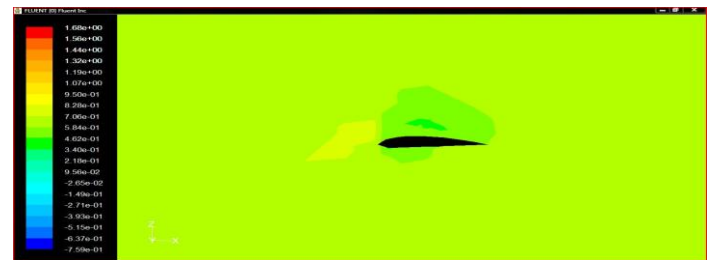


**Figure 6.13 (PRESSURE DISTRIBUTION OF BLADE AT BLADE TIP)**

The above figure 6.13 is the pressure distribution at blade tip. In blade tip normally pressure is more or less same in all faces.

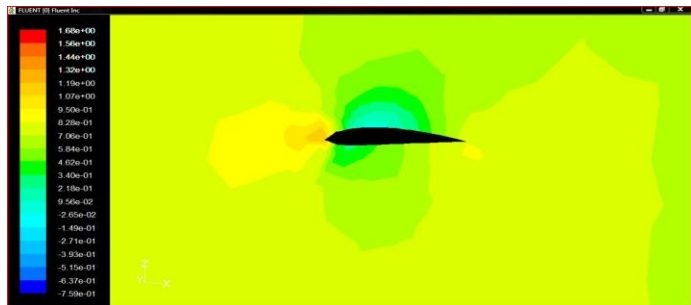


**Figure 6.11 (PRESSURE DISTRIBUTION OF BLADE AT 5.5M)**

The above figure 6.11 is pressure distribution of Iso-surface of blade in 5.5m from bottom. In the above figure the maximum pressure (stagnation pressure) occurs on the leading edge of the aerofoil shape and minimum pressure occurs in upper surface of the aerofoil shape

**6.1.2. FLAP WITH 10<sup>0</sup> DOWNWARD DEFLECTION**

Import the NACA4415 vertex data in different chord length (1.05C at tip of the blade, 1.293253C at 8m from tip of the blade and 2.1C at bottom of blade). The distance between the tip and bottom aerofoil is 34.5m and distance from the tip to middle aerofoil is 8m. And deflect the middle aerofoil at 10<sup>0</sup> downward Z-axis (by using copy & rotate). Joint the vertex points and create an aerofoil. Now connect the leading and trailing edges of the aerofoils. This shape looks like an aircraft wing. After the finishing of connection aerofoil we start to draw a cylinder with height 3m and radius 0.5m from the origin (0, 0, and 0). Now we connect the wing to the cylinder (the distance between wing and cylinder is 2.5m). And we get wind turbine blade without flap. After creating the blade model does the facing process after that does the volume process. Now get a single volume.

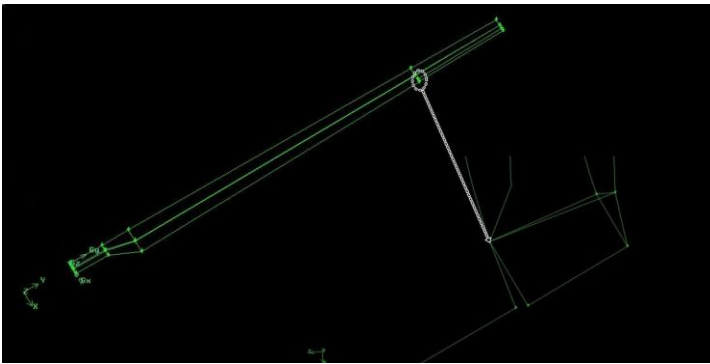


**Figure 6.14** (SINGLE VOLUME BLADE WITH FLAP AT 10°)

Now we need to create the control volume with the dimension of height 80m (+ve Y-direction), length 80m (60m from centre of cylinder in the direction of +ve X-direction, 20m from centre of cylinder in the -ve X-direction) and dept40m (20m in +ve Z-direction and 20m in -ve Z-direction). After finishing the creation of control volume subtract the blade volume into control volume. Now we get a single volume.

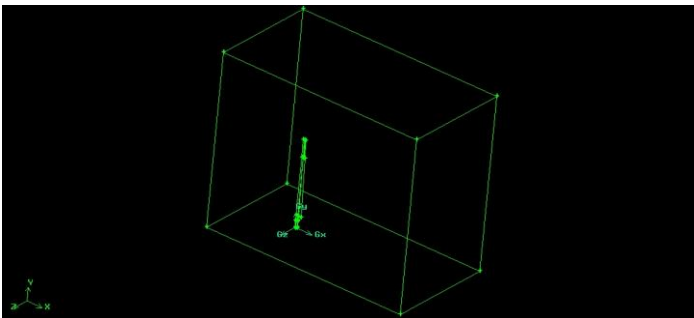


**Figure 6.15** (BLADE WITH FLAP 10° DEFLECTED WITH CONTROL VOLUME)

After finishing the volume process we need do the meshing process. First mesh the each line in the model and after finishing the line mesh, mesh the each face mesh. After finishing the face mesh, mesh the full volume by using volume mesh. After the meshing process export the model in the “.msh” format.

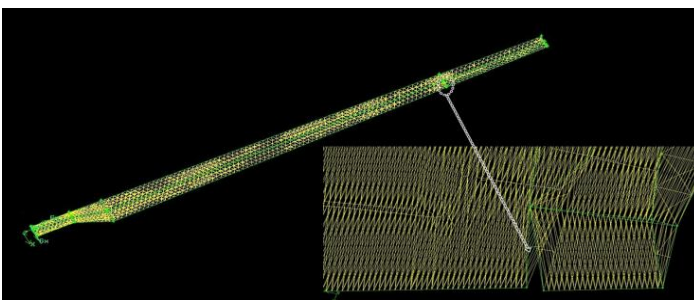


**Figure 6.16.a.** (MESHED BLADE WITH FLAP 20° DEFLECTED)

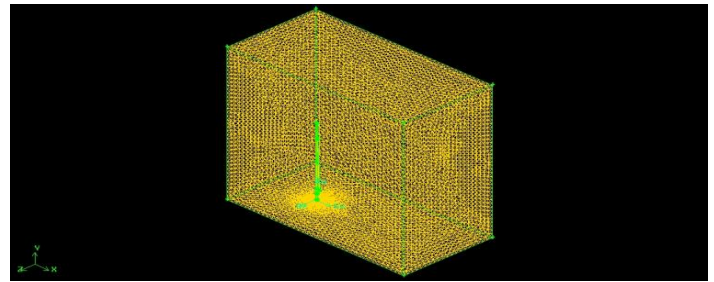


**Figure 6.16.b.** (MESHED BLADE WITH FLAP 20° DEFLECTED WITH CONTROL VOLUME)

After the modeling the 3D blade we need to analysis the aerodynamic efficiency by using the FLUENT. Read the “.msh” file in the FLUENT and follow the steps which already discussed in chapter3.after finishing the “iterate” process create the Iso-Surface in distance 3m, 4m, 5.5m, 20m and 40m from origin and click the contours in display option and see the result of velocity of fluid flow through the model.

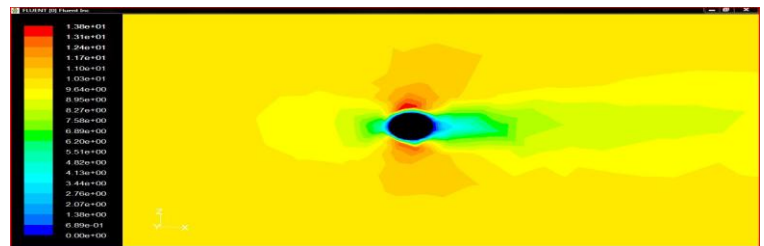


**Figure 6.17** (VELOCITY DISTRIBUTION OF BLADE AT 3M)

The above figure 6.17 is velocity distribution of Iso-surface of blade in 3m from bottom. In the above figure the maximum velocity occurs on upper surface of circle and the minimum velocity occurs in trailing edge of the cylinder. The below figure 6.18 is velocity distribution of Iso-surface of blade in 4m from bottom. It is the in between volume of cylinder and wing. In the above figure the maximum velocity occurs on upper and lower surface and the minimum velocity occurs in trailing edge of the cut section and in the leading edge velocity also low. The figure 6.19 is the velocity distribution of cut section of blade at 5.5m from the bottom. Here the maximum velocity occurs on the upper surface of the blade and the velocity minimum at leading edge and trailing edges of the blade.

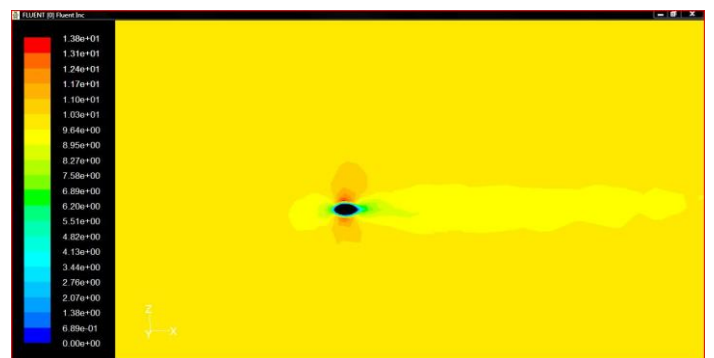


**Figure 6.18** (VELOCITY DISTRIBUTION OF BLADE AT 4M)

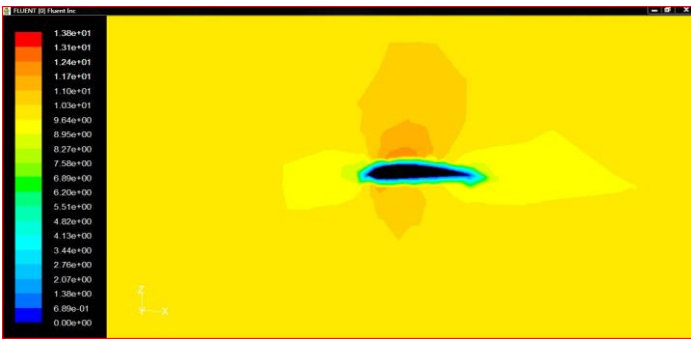


**Figure 6.19** (VELOCITY DISTRIBUTION OF BLADE AT 5.5M)

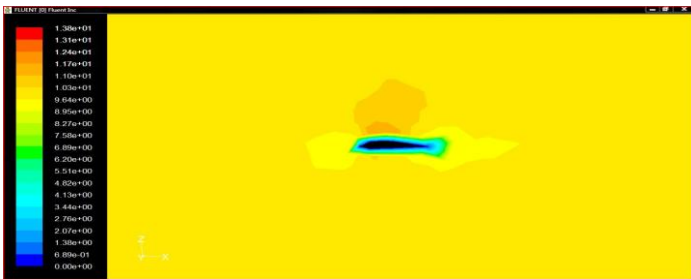


**Figure 6.20** (VELOCITY DISTRIBUTION OF BLADE AT 20M)

The above figure 6.20 is the velocity distribution of cut section of blade at 20m from the bottom. Here the maximum velocity occurs on the upper surface and other surface in this cut section the velocity is low compare than upper velocity in surface.

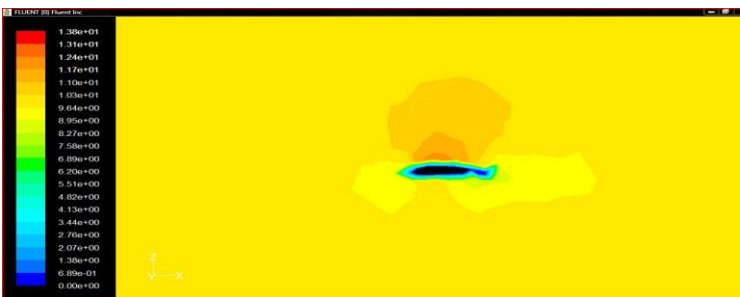


**Figure 6.21** (VELOCITY DISTRIBUTION OF BLADE AT 32M)

The above figure 6.21 is the velocity distribution of cut section of blade at 32m from the bottom at point which the flap is attached. Here the maximum velocity occurs on the upper surface and other surface in this cut section the velocity is same and low compare than upper velocity in surface.

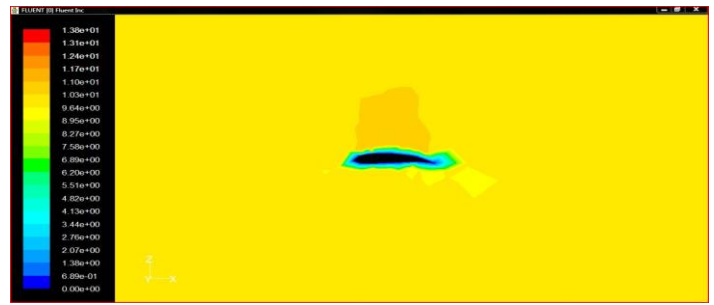


**Figure 6.22** (VELOCITY DISTRIBUTION OF BLADE AT BLADE TIP)

The above figure 6.22 is the velocity distribution at blade tip. In blade tip normally velocity is more or less same in all faces in the tip. And for pressure distribution click the contours in display option and select the Iso-surfaces and see the result of pressure of fluid flow through the model. The below figure 6.23 is pressure distribution of Iso-surface of blade in 3m from bottom. In the above figure the maximum pressure (stagnation pressure) occurs in leading edge of circle and the minimum velocity occurs on trailing upper and lower surface of the cylinder.

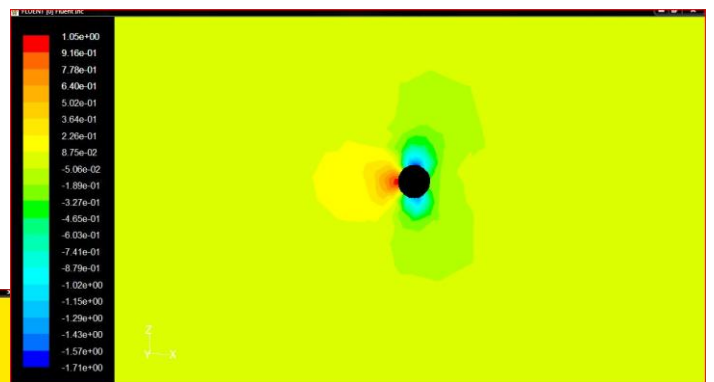


**FIGURE 6.23** (PRESSURE DISTRIBUTION OF BLADE AT 3M)

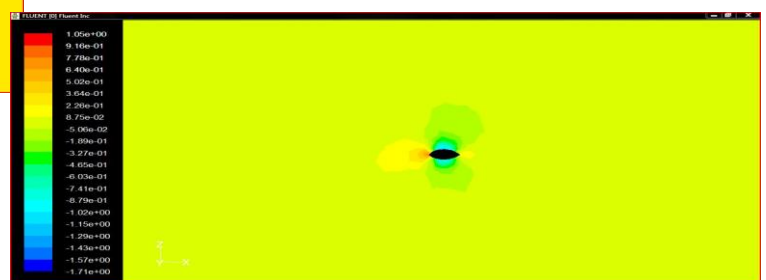


**Figure 6.24** (PRESSURE DISTRIBUTION OF BLADE AT 4M)

The above figure 6.24 is pressure distribution of Iso-surface of blade in 4m from bottom. In the above figure the maximum pressure (stagnation pressure) occurs on the leading edge of the surface and minimum pressure occurs in upper and lower surface.



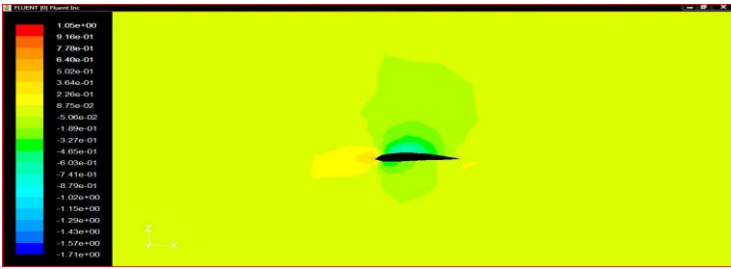


**Figure 6.25 (PRESSURE DISTRIBUTION OF BLADE AT 5.5M)**

The above figure 6.25 is pressure distribution of Iso-surface of blade in 5.5m from bottom. In the above figure the maximum pressure occurs on the leading edge of the aerofoil shape and minimum pressure occurs in upper surface of the aerofoil shape

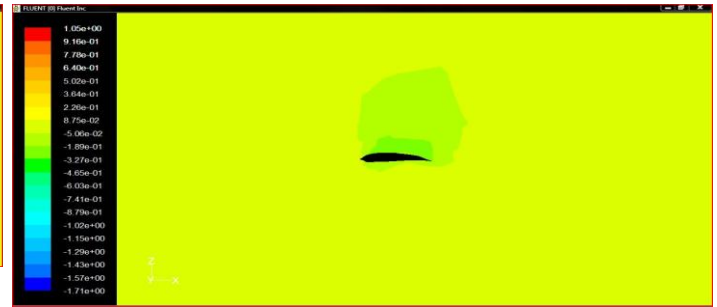


**Figure 6.28 (PRESSURE DISTRIBUTION OF BLADE AT BLADE TIP)**

The above figure 6.28 is the pressure distribution at blade tip. In blade tip normally pressure is more or less same in all faces.

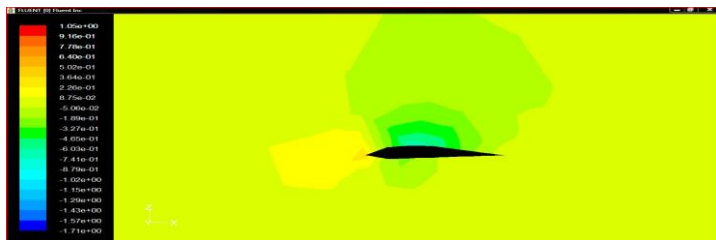


**Figure 6.26 (PRESSURE DISTRIBUTION OF BLADE AT 20 M)**

The above figure 6.26 is pressure distribution of Iso-surface of blade in 20m from bottom. In the above figure the maximum pressure occurs on the leading edge of the aerofoil shape and minimum pressure occurs in upper surface of the aerofoil shape.

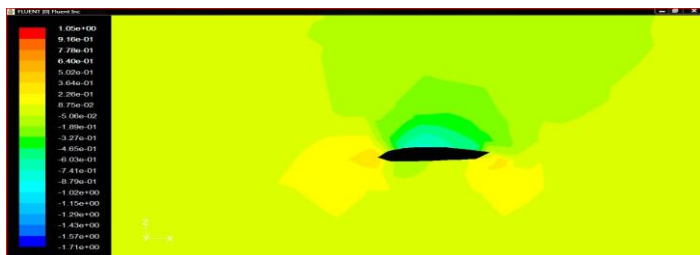


**Figure 6.27 (PRESSURE DISTRIBUTION OF BLADE AT 32M)**

The above figure 6.27 is the pressure distribution of cut section of blade at 32m from the bottom at point which the flap is attached. Here the maximum pressure occurs on the leading and trailing edges in the upper surface the pressure is very low.

**6.1.3. FLAP WITH 20° DOWNWARD DEFLECTION**

Import the NACA4415 vertex data in different chord length (1.05C at tip of the blade, 1.293253C at 8m from tip of the blade and 2.1C at bottom of blade). The distance between the tip and bottom aerofoil is 34.5m and distance from the tip to middle aerofoil is 8m. And deflect the middle aerofoil at 10° downward Z-axis (by using copy & rotate). Joint the vertex points and create an aerofoil. Now connect the leading and trailing edges of the aerofoils. This shape looks like an aircraft wing. After the finishing of connection aerofoil we start to draw a cylinder with height 3m and radius 0.5m from the origin (0, 0, 0, and 0). Now we connect the wing to the cylinder (the distance between wing and cylinder is 2.5m). And we get wind turbine blade without flap. After creating the blade model does the facing process after that does the volume process. Now get a single volume.

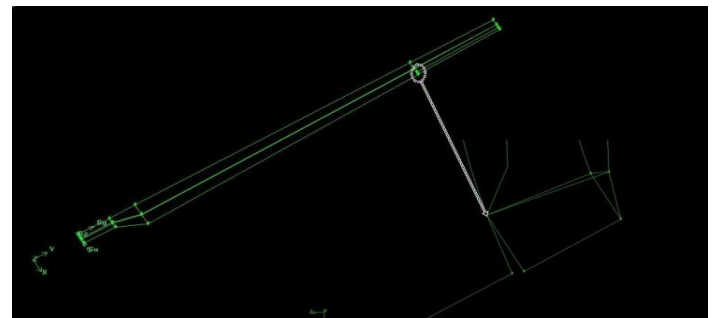


**Figure 6.29 (SINGLE VOLUME BLADE WITH FLAP AT 20°)**

Now we need to create the control volume with the dimension of height 80m (+ve Y-direction), length 80m (60m from centre of cylinder in the +ve X-direction, 20m from centre of cylinder in the -ve X-direction) and depth 40m (20m in +ve Z-direction and 20m in -ve Z-direction). After finishing the creation of control volume subtract the blade volume into control volume. Now we get a single volume.

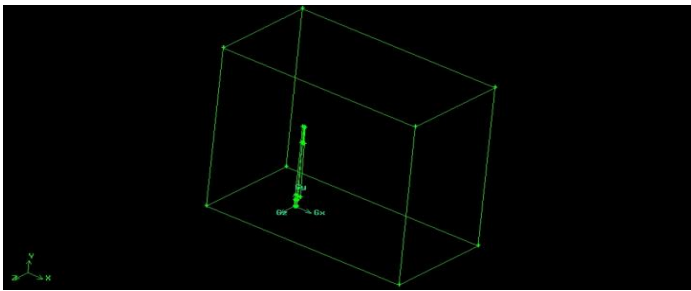


**Figure 6.29 (FLAP 20° DEFLECTED BLADE WITH CONTROL VOLUME)**

After finishing the volume process we need do the meshing process. First mesh the each line in the model and after finishing the line mesh, mesh the each face mesh. After finishing the face mesh, mesh the full volume by using volume mesh. After the meshing process export the model in the “.msh” format.

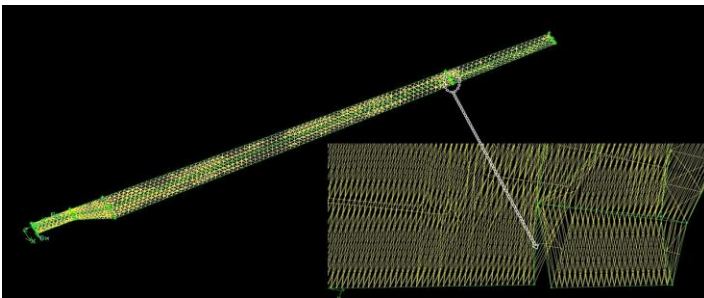


**Figure 6.30.a. (MESHED BLADE WITH FLAP 20° DEFLECTED)**

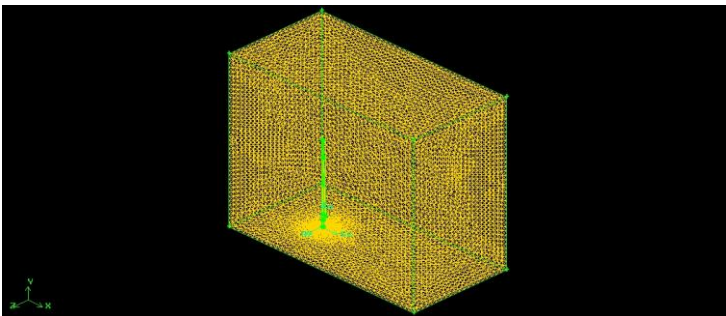


**Figure 6.30.b. (MESHED BLADE WITH FLAP 20° DEFLECTED WITH CONTROL VOLUME)**

After the modeling the 3D blade we need to analysis the aerodynamic efficiency by using the FLUENT. Read the “.msh” file in the FLUENT and follow the steps which already discussed in chapter3.after finishing the “iterate” process create the Iso-Surface in distance 3m, 4m, 5.5m, 20m and 40m from origin and click the contours in display option and see the result of velocity of fluid flow through the model.

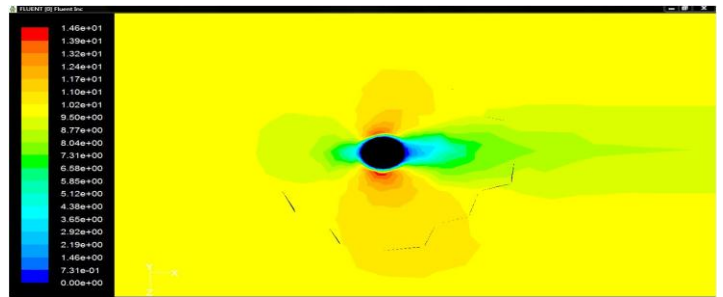


**Figure 6.31 (VELOCITY DISTRIBUTION OF BLADE AT 3M)**

The above figure 6.31 is velocity distribution of Iso-surface of blade in 3m from bottom. In the above figure the maximum velocity occurs on upper surface of circle and the minimum velocity occurs in trailing edge of the cylinder. Compare than upper surface the velocity is high in lower surface.

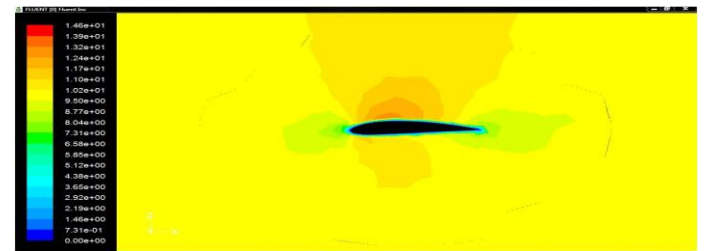


**Figure 6.32 (VELOCITY DISTRIBUTION OF BLADE AT 5.5M)**

The figure 6.32 is the velocity distribution of cut section of blade at 5.5m from the bottom. Here the maximum velocity occurs on the upper surface of the blade and the velocity minimum at leading edge and trailing edges of the blade. The above figure 6.33 is the velocity distribution of cut section of blade at 20m from the bottom. Here the maximum velocity occurs on the upper surface and other surface in this cut section the velocity is low compare than upper velocity in surface. The above figure 6.34 is the velocity distribution of cut section of blade at 30m from the bottom. Here the maximum velocity occurs on the upper surface and other surface in this cut section the velocity is same and low compare than upper velocity in surface.

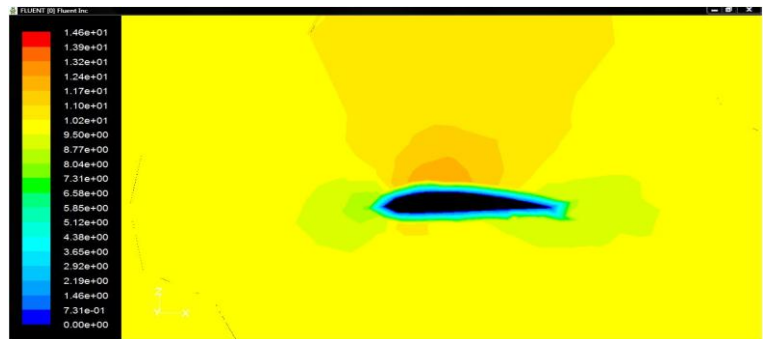


**Figure 6.33 (VELOCITY DISTRIBUTION OF BLADE AT 20M)**

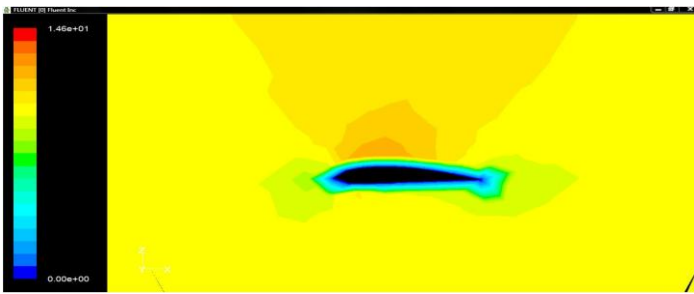


**Figure 6.34 (VELOCITY DISTRIBUTION OF BLADE AT 30M)**

The below figure 6.35 is the velocity distribution of cut section of blade at 35m from the bottom, and in this section flap is attached. Here the maximum velocity occurs on the upper surface and other surface in this cut section the velocity is same and low compare than upper velocity in surface.

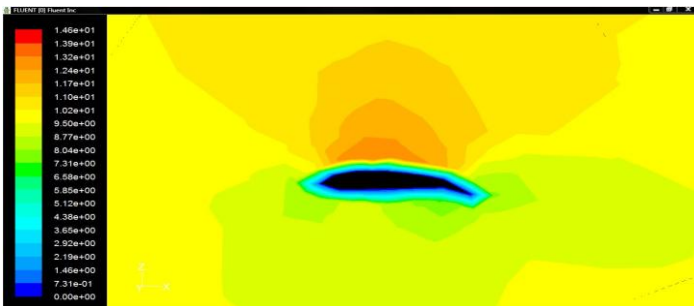


**Figure 6.35 (VELOCITY DISTRIBUTION OF BLADE AT 35M)**

The below figure 6.36 is the velocity distribution at blade tip. In blade tip normally velocity is more or less same in all faces in the tip.

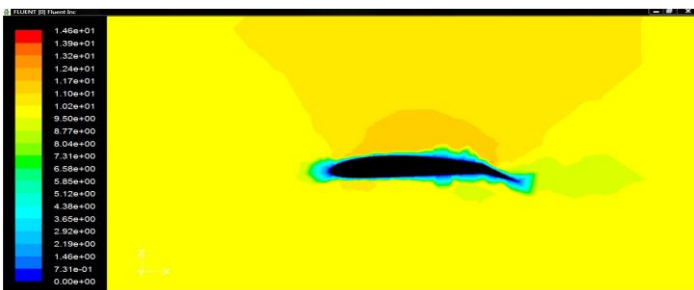


**Figure 6.36 (VELOCITY DISTRIBUTION OF BLADE AT BLADE TIP)**

And for pressure distribution click the contours in display option and select the Iso-surfaces and see the result of pressure of fluid flow through the model.

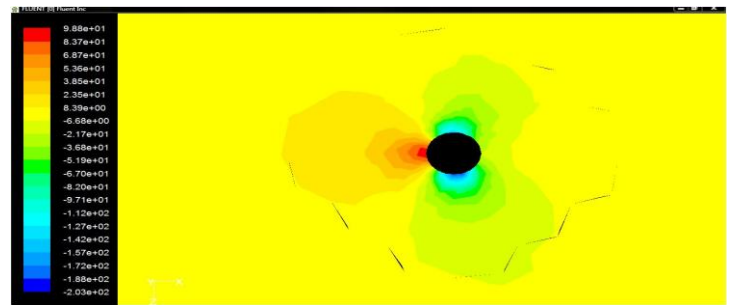


**Figure 6.37 (PRESSURE DISTRIBUTION OF BLADE AT 3M)**

The above figure 6.37 is pressure distribution of Iso-surface of blade in 3m from bottom. In the above figure the maximum pressure (stagnation pressure) occurs in leading edge of circle and the minimum velocity occurs on trailing upper and lower surface of the cylinder. The below figure 6.38 is pressure distribution of Iso-surface of blade in 5.5m from bottom. In the below figure the maximum pressure occurs on the leading edge of the aerofoil shape and minimum pressure occurs in upper surface of the aerofoil shape. The below figure 6.39 is pressure distribution of Iso-surface of blade in 20m from bottom. In the below figure the maximum pressure occurs on the leading edge of the aerofoil shape and minimum pressure occurs in upper surface of the aerofoil shape.

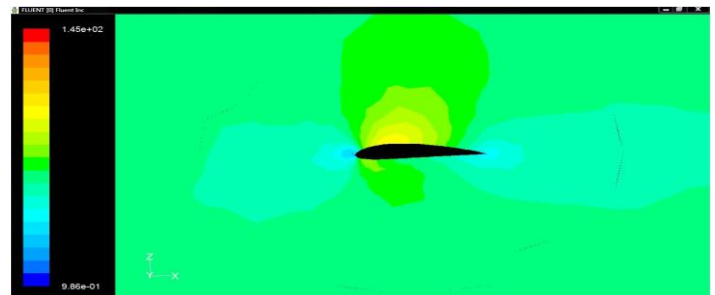


**Figure 6.38 (VELOCITY DISTRIBUTION OF BLADE AT 5.5M)**

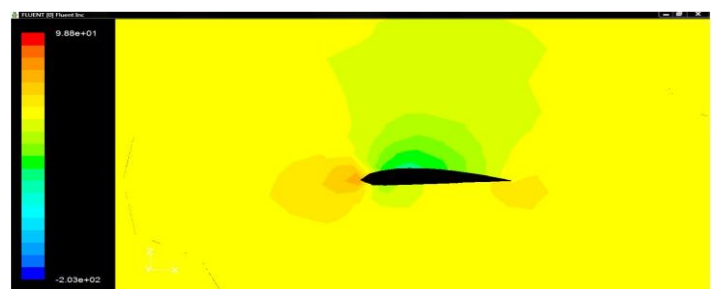


**Figure 6.39 (VELOCITY DISTRIBUTION OF BLADE AT 20M)**



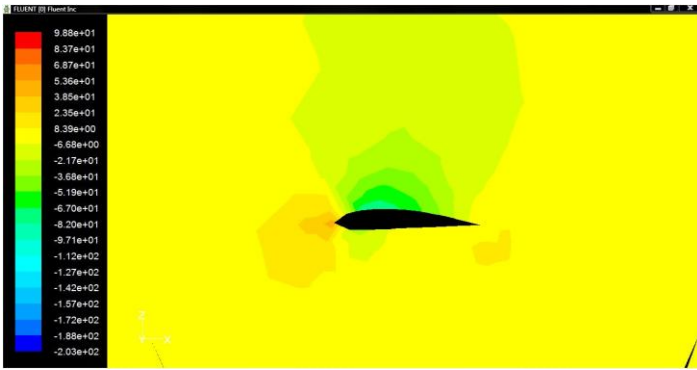


Figure 6.40 (VELOCITY DISTRIBUTION OF BLADE AT 30M)

The above figure 6.40 is the pressure distribution of cut section of blade at 30m from the bottom. Here the maximum pressure occurs on the leading and trailing edges in the upper surface the pressure is very low.

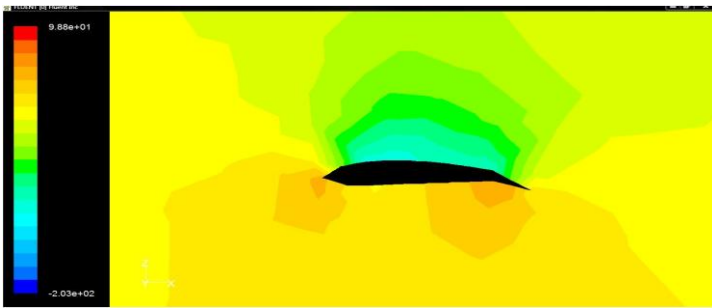


Figure 6.41 (VELOCITY DISTRIBUTION OF BLADE AT 35M)

The above figure 6.41 is the pressure distribution of cut section of blade at 35m from the bottom, and in this section flap is attached. Here the maximum pressure occurs on the leading and trailing edges in the upper surface the pressure is very low.

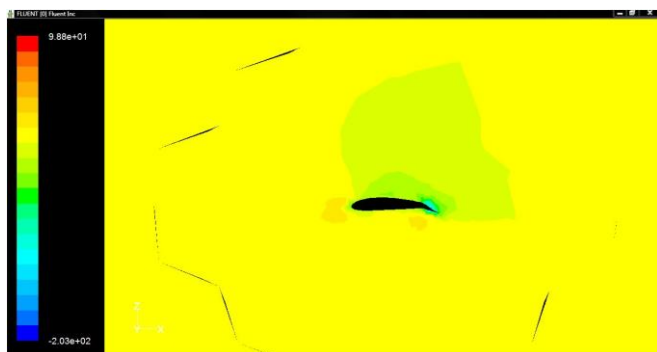


Figure 6.42 (VELOCITY DISTRIBUTION OF BLADE AT BLADE TIP)

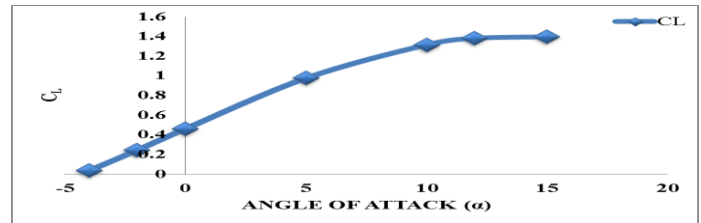
The above figure 6.42 is the pressure distribution at blade tip. In blade tip normally pressure is more or less same in all faces. And the pressure is very low on the upper & lower surface of the flap. In this chapter we clearly understand, how the pressure and velocity was varied with & without flap.

## 7. RESULT AND DISCUSSIONS

In the present work, the using of flap in the wind turbine blade is increasing of lift co-efficient and also the drag co-efficient is increased in little amount. But the amount of drag co-efficient very small with compare then the amount increasing lift co-efficient. Hence there is a sufficient increase in the L/D ratio that is aerodynamic efficiency. In this chapter we will discuss about co-efficient of lift, co-efficient of drag, co-efficient of lift to drag ratio and co-efficient of pressure of the wind turbine model (2D & 3D) with and without flap with different angle of attack (AOA).

### 7.1. LIFT CO-EFFICIENT FOR 2D MODELS

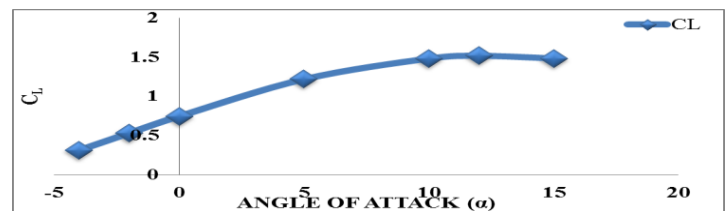
#### 7.1.1. $C_L$ VS $\alpha$ FOR WITHOUT FLAP



Graph 7.1 ( $C_L$  VS  $\alpha$  FOR WITHOUT FLAP)

The above graph is plot co-efficient of lift for different angle of attack. The  $C_L$  is gradually increased with the angle of attack increases. From the figure 5.3 the velocity in the upper surface is high. So in the lower surface the pressure is high. Due to the high pressure the lift is created. The lift is increased with the increase of angle of attack.

#### 7.1.2. $C_L$ VS $\alpha$ FOR WITH FLAP AT DEFLECTED 5° DOWNWARD DIRECTION

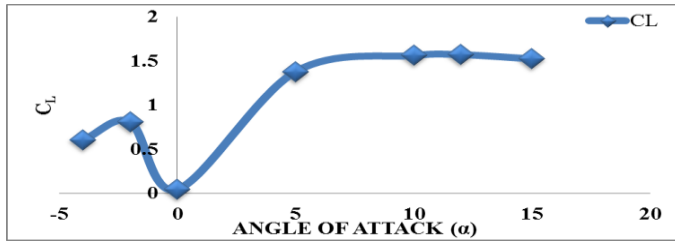


Graph 7.2 ( $C_L$  VS  $\alpha$  FOR WITH FLAP AT DEFLECTED 5° DOWNWARD DIRECTION)

The above graph is plot co-efficient of lift for different angle of attack. The  $C_L$  is gradually increased with the angle of attack increases. From the figure 5.11 the velocity in the upper surface is high. So in the lower surface the pressure is high. Due to the high pressure the lift is created. The lift is increased with the increase of angle of attack. A trailing edge flap is simply a portion of the trailing edge section of the aerofoil that is hinged and which can be deflected downward, as sketched in the insert in Graph 7.2. The positive angle 5° in Graph 7.1, the lift co-efficient is increased (compare the Graph 7.1 with Graph 7.2). This increase is due to an effective increase in the camber of the aerofoil as the flap is deflected downward. In the Graph 7.1 the lift co-efficient is very less at minimum angle of attack -4° (less than 0.1) but in the Graph 7.2 the lift co-efficient at minimum angle of attack -4° is near than 0.3. It is high compare than blade without flap.

And also the maximum lift co-efficient of blade without flap is 1.4 at angle of attack +20°. It is also less compare than blade with flap. The maximum lift co-efficient of blade with flap at 5° deflected is 1.5 at angle of attack +20°.

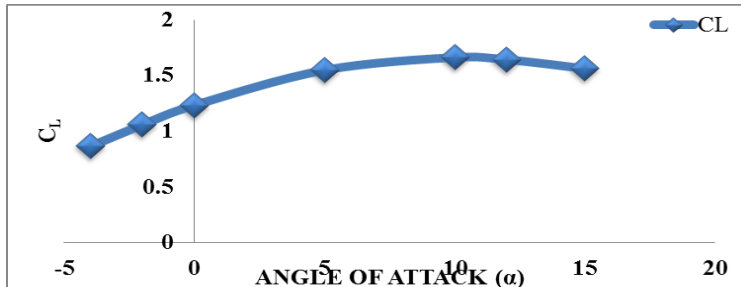
**7.1.3.  $C_L$  VS  $\alpha$  FOR WITH FLAP AT DEFLECTED 10° DOWNWARD DIRECTION**



**Graph 7.3 ( $C_L$  VS  $\alpha$  FOR WITH FLAP AT DEFLECTED 10° DOWNWARD DIRECTION)**

The above graph is plot co-efficient of lift for different angle of attack. The  $C_L$  is gradually increased with the angle of attack increases. From the Graph 5.19 the velocity in the upper surface is high. So in the lower surface the pressure is high. Due to the high pressure the lift is created. The lift is increased with the increase of angle of attack. A trailing edge flap is simply a portion of the trailing edge section of the aerofoil that is hinged and which can be deflected downward, as sketched in the insert in Graph 7.3. The positive angle 10° in Graph 7.3, the lift co-efficient is increased (compare the Graph 7.1 & Graph 7.2 with 7.3). This increase is due to an effective increase in the camber of the aerofoil as the flap is deflected downward. In the Graph 7.1 the lift co-efficient is very less at minimum angle of attack -4° (less than 0.1) and in the Graph 7.2 the lift co-efficient at minimum angle of attack -4° is near than 0.3 but in Graph 7.3 the lift co-efficient at minimum angle of attack -4° is near than 0.5. It is high compare than blade without flap and also the blade with flap deflected 5°. And also the maximum lift co-efficient of blade without flap is 1.4 at angle of attack +20°. It is also less compare than blade with flap. The maximum lift co-efficient of blade with flap at 10° deflected is more than 1.5 at angle of attack +20° and it is also high compare then the blade with flap deflected 5°. In the Graph 7.3 the lift co-efficient at angle of attack 0° is suddenly deviated (decreased) from our expectation. It may be occurs due to the problem in meshing of the aerofoil or geometrical error or computational problem.

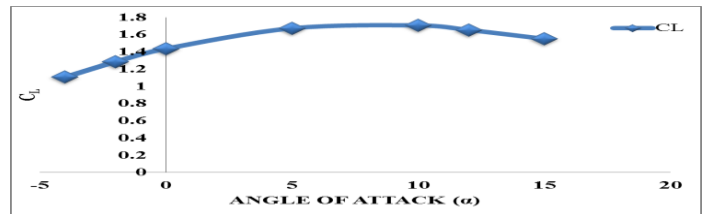
**7.1.4.  $C_L$  VS  $\alpha$  FOR WITH FLAP AT DEFLECTED 15° DOWNWARD DIRECTION**



**Graph 7.4 ( $C_L$  VS  $\alpha$  FOR WITH FLAP AT DEFLECTED 15° DOWNWARD DIRECTION)**

The above graph is plot co-efficient of lift for different angle of attack. The  $C_L$  is gradually increased with the angle of attack increases. From the figure 5.19 the velocity in the upper surface is high. So in the lower surface the pressure is high. Due to the high pressure the lift is created. The lift is increased with the increase of angle of attack. The positive angle 15° in Graph 7.4, the lift co-efficient is increased (compare the Graph 7.1 & Graph 7.2 with 7.4 but nearly equal to the Graph 7.3). This increase is due to an effective increase in the camber of the aerofoil as the flap is deflected downward. In the Graph 7.4 the lift co-efficient is very high (more than 0.8) at minimum angle of attack -4° with compare than Graph 7.1, 7.2 & 7.3. And also the maximum lift co-efficient more than 1.5 at angle of attack +20°. It is also more than  $C_L$  of blade without flap,  $C_L$  of blade with flap with deflected 5° &  $C_L$  of blade with flap deflected 10°.

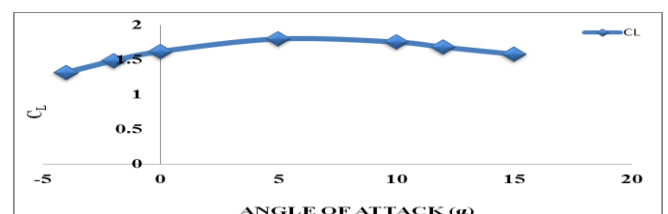
**7.1.5.  $C_L$  VS  $\alpha$  FOR WITH FLAP AT DEFLECTED 20° DOWNWARD DIRECTION**



**Graph 7.5 ( $C_L$  VS  $\alpha$  FOR WITH FLAP AT DEFLECTED 20°)**

The above graph is plot co-efficient of lift for different angle of attack. The  $C_L$  is gradually increased with the angle of attack increases. From the Graph 5.35 the velocity in the upper surface is high. So in the lower surface the pressure is high. Due to the high pressure the lift is created. The lift is increased with the increase of angle of attack. A trailing edge flap is simply a portion of the trailing edge section of the aerofoil that is hinged and which can be deflected downward, as sketched in the insert in Graph 7.5. The positive angle 20° in Graph 7.5, the lift co-efficient is increased (compare the Graph 7.1, 7.2, 7.3 & 7.4 with Graph 7.5). This increase is due to an effective increase in the camber of the aerofoil as the flap is deflected downward. In the Graph 7.5 the lift co-efficient is very high (more than 1) at minimum angle of attack -4° with compare than Graph 7.1, 7.2, 7.3 & 7.4. And also the maximum lift co-efficient more than 1.5 at angle of attack +20°. It is also more than  $C_L$  of blade without flap,  $C_L$  of blade with flap with deflected 5° and also equal to the  $C_L$  of blade with flap deflected 10° and  $C_L$  of blade with flap deflected 15°.

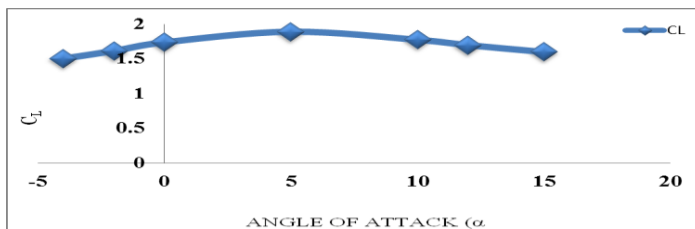
**7.1.7.  $C_L$  VS  $\alpha$  FOR WITH FLAP AT DEFLECTED 25° DOWNWARD DIRECTION**



**Graph 7.6 ( $C_L$  VS  $\alpha$  FOR WITH FLAP AT DEFLECTED 25° DOWNWARD DIRECTION)**

The above graph is plot co-efficient of lift for different angle of attack. The  $C_L$  is gradually increased with the angle of attack increases. From the figure 5.39 the velocity in the upper surface is high. So in the lower surface the pressure is high. Due to the high pressure the lift is created. The lift is increased with the increase of angle of attack. A trailing edge flap is simply a portion of the trailing edge section of the aerofoil that is hinged and which can be deflected downward, as sketched in the insert in Graph 7.7. The positive angle  $25^\circ$  in Graph 7.6, the lift co-efficient is increased (compare the Graph 7.1, 7.2, 7.3, 7.4 & 7.5 with Graph 7.6). This increase is due to an effective increase in the camber of the aerofoil as the flap is deflected downward. In the Graph 7.6 the lift co-efficient is very high (more than 1.2) at minimum angle of attack  $-4^\circ$  with compare than Graph 7.1, 7.2, 7.3, 7.4 & 7.5. And also the maximum lift co-efficient more than 1.5 at angle of attack  $+20^\circ$ . It is also more than  $C_L$  of blade without flap,  $C_L$  of blade with flap with deflected  $5^\circ$  and also equal to the  $C_L$  of blade with flap deflected  $10^\circ$ ,  $C_L$  of blade with flap deflected  $15^\circ$  and  $C_L$  of blade with flap deflected  $20^\circ$

### 7.1.7. $C_L$ VS $\alpha$ FOR WITH FLAP AT DEFLECTED $30^\circ$ DOWNWARD DIRECTION

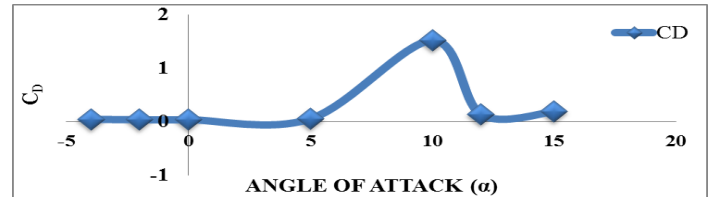


**Graph 7.7** ( $C_L$  VS  $\alpha$  FOR WITH FLAP AT DEFLECTED  $30^\circ$  DOWNWARD DIRECTION)

The above graph is plot co-efficient of lift for different angle of attack. The  $C_L$  is gradually increased with the angle of attack increases. From the Graph 5.43 the velocity in the upper surface is high. So in the lower surface the pressure is high. Due to the high pressure the lift is created. The lift is increased with the increase of angle of attack. A trailing edge flap is simply a portion of the trailing edge section of the aerofoil that is hinged and which can be deflected downward, as sketched in the insert in Graph 7.7. The positive angle  $30^\circ$  in Graph 7.7, the lift co-efficient is increased (compare the Graph 7.1, 7.2, 7.3, 7.4, 7.5 & 7.6 with Graph 7.7). This increase is due to an effective increase in the camber of the aerofoil as the flap is deflected downward. In the Graph 7.6 the lift co-efficient is very high (more than 1.4) at minimum angle of attack  $-4^\circ$  with compare than Graph 7.1, 7.2, 7.3, 7.4, 7.5 & 7.7. And also the maximum lift co-efficient more than 1.5 at angle of attack  $+20^\circ$ . It is also more than  $C_L$  of blade without flap,  $C_L$  of blade with flap with deflected  $5^\circ$  and also equal to the  $C_L$  of blade with flap deflected  $10^\circ$ ,  $C_L$  of blade with flap deflected  $15^\circ$ ,  $C_L$  of blade with flap deflected  $20^\circ$  and  $C_L$  of blade with flap deflected  $25^\circ$

## 7.2. DRAG CO-EFFICIENT FOR 2D MODELS

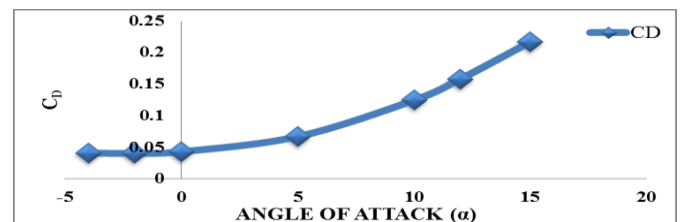
### 7.2.1. $C_D$ VS $\alpha$ FOR WITHOUT FLAP



**Graph 7.8** ( $C_D$  VS  $\alpha$  FOR WITHOUT FLAP)

The above graph is plot co-efficient of drag for different angle of attack. The  $C_D$  is gradually increased with the angle of attack increases. From the figure 5.3 the velocity in the upper surface is high. So in the lower surface the pressure is high. Due to the high pressure the lift is created. The lift is increased with the increase of angle of attack. Due to that the flow separation occurs in the trailing edge. So the pressure drag is increased in trailing edge and the skin friction drag increased in the lower surface. The physical source of this drag co-efficient is both skin friction drag and pressure drag due to flow separation (so called from drag). The sum of these two effect yields the profile drag co-efficient  $C_D$  for the aerofoil, which is plotted in Graph7.8. The drag is increased with the increase of lift. The wake is created due to the increase of the angle of attack. So the drag is increased. Both  $C_L$  and  $C_D$  are increased in the increase of angle of attack (AOA). In the Graph 7.6 the drag co-efficient at angle of attack  $10^\circ$  is suddenly deviated (increased) from our expectation. It may be occurs due to the problem in meshing of the aerofoil or geometrical error or computational problem.

### 7.2.2. $C_D$ VS $\alpha$ FOR WITH FLAP AT DEFLECTED $5^\circ$ DOWNWARD DIRECTION



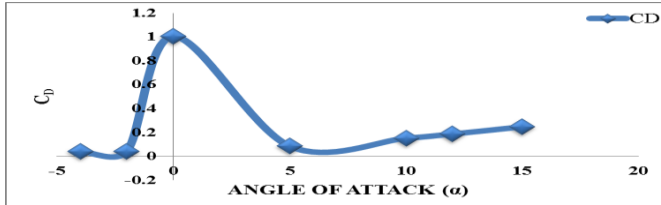
**Graph 7.9** ( $C_D$  VS  $\alpha$  FOR WITH FLAP AT DEFLECTED  $5^\circ$  DOWNWARD DIRECTION)

The above is the co-efficient of drag for different angle of attack for wind turbine blade with flap at deflected  $5^\circ$ . We can clearly understand the drag increased with increase of angle of attack. A trailing edge flap is simply a portion of the trailing edge section of the aerofoil that is hinged and which can be deflected downward, as sketched in the insert in Graph 7.7. The positive angle  $5^\circ$  in Graph 7.9, the drag co-efficient is increased (compare the Graph 7.8 with Graph 7.9). This increase is due to an effective increase in the camber of the aerofoil as the flap is deflected downward. Due to an effective in the camber the flow separation is also increased. In the increment of flow separation the pressure drag is increased and also the skin frictions drag. Then the net drag is increased. So the drag co-efficient is increases with the flow angle of attack. In the Graph 7.8 the drag co-efficient is very less at minimum angle of attack  $-4^\circ$  (less than 0.01) but in the Graph 7.9 the drag co-efficient at minimum angle of attack  $-4^\circ$  is near than 0.04. It is high compare than blade without flap.



And also the maximum drag co-efficient of blade without flap is 0.2 at angle of attack  $+15^\circ$ . It is also less compare than blade with flap. The maximum lift co-efficient of blade with flap at  $5^\circ$  deflected is 0.221 at angle of attack  $+15^\circ$ .

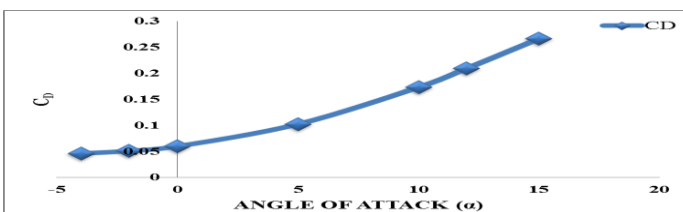
### 7.2.3. $C_D$ VS $\alpha$ FOR WITH FLAP AT DEFLECTED $10^\circ$ DOWNWARD DIRECTION



**Graph 7.10** ( $C_D$  VS  $\alpha$  FOR WITH FLAP AT DEFLECTED  $10^\circ$  DOWNWARD DIRECTION)

The above is the co-efficient of drag for different angle of attack for wind turbine blade with flap at deflected  $10^\circ$ . We can clearly understand the drag increased with increase of angle of attack. In the above Graph 7.10 the drag co-efficient at angle of attack  $0^\circ$  is suddenly deviated (increased) from our expectation. It may be occurs due to the problem in meshing of the aerofoil or geometrical error or computational problem. In the Graph 7.8 the drag co-efficient is very less at minimum angle of attack  $-4^\circ$  (less than 0.01) and in the Graph 7.9 the drag co-efficient at minimum angle of attack  $-4^\circ$  is near than 0.04 but and in the Graph 7.9 the drag co-efficient at minimum angle of attack  $-4^\circ$  is near than 0.05. It is high compare than blade without flap. And also the maximum drag co-efficient of blade without flap deflected with  $10^\circ$  is near than 0.3 at angle of attack  $+15^\circ$ . It is also more compare than blade with flap at  $5^\circ$  and blade without flap.

### 7.2.4. $C_D$ VS $\alpha$ FOR WITH FLAP AT DEFLECTED $15^\circ$ DOWNWARD DIRECTION

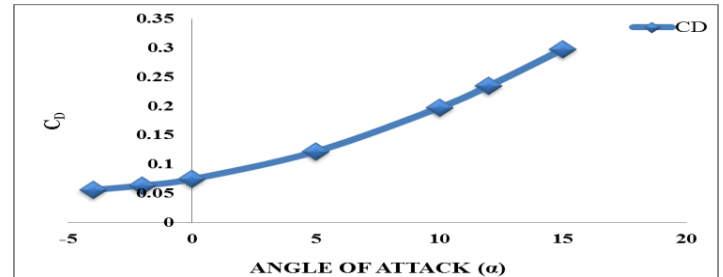


**Graph 7.11** ( $C_D$  VS  $\alpha$  FOR WITH FLAP AT DEFLECTED  $15^\circ$  DOWNWARD DIRECTION)

The above is the co-efficient of drag for different angle of attack for wind turbine blade with flap at deflected  $15^\circ$ . We can clearly understand the drag increased with increase of angle of attack. A trailing edge flap is simply a portion of the trailing edge section of the aerofoil that is hinged and which can be deflected downward, as sketched in the insert in Graph 7.11. The positive angle  $15^\circ$  in Graph 7.11, the drag co-efficient is increased (compare the Graph 7.8, Graph 7.9 and Graph 7.10 with Graph 7.11). This increase is due to an effective increase in the camber of the aerofoil as the flap is deflected downward. Due to an effective in the camber the flow separation is also increased. In the increment of flow separation the pressure drag is increased and also the skin

frictions drag. Then the net drag is increased. So the drag co-efficient is increases with the flow angle of attack. The above Graph 7.11 the drag co-efficient at the angle of attack  $+15^\circ$  is more 0.25 it is more than the  $C_D$  of blade without flap, flap with  $5^\circ$  and flap with  $10^\circ$ .

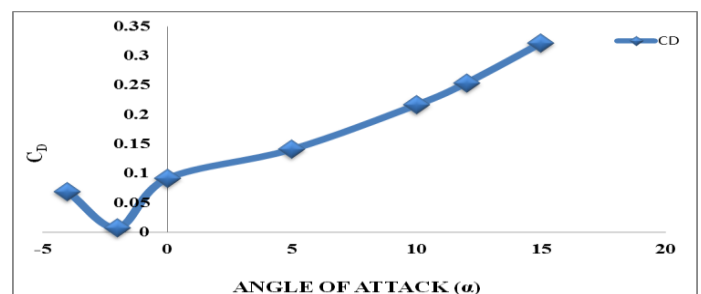
### 7.2.5. $C_D$ VS $\alpha$ FOR WITH FLAP AT DEFLECTED $20^\circ$ DOWNWARD DIRECTION



**Graph 7.12** ( $C_D$  VS  $\alpha$  FOR WITH FLAP AT DEFLECTED  $20^\circ$  DOWNWARD DIRECTION)

The above is the co-efficient of drag for different angle of attack for wind turbine blade with flap at deflected  $20^\circ$ . We can clearly understand the drag increased with increase of angle of attack. A trailing edge flap is simply a portion of the trailing edge section of the aerofoil that is hinged and which can be deflected downward, as sketched in the insert in Graph 7.12. The positive angle  $10^\circ$  in Graph 7.12, the drag co-efficient is increased (compare the Graph 7.8, Graph 7.9 and Graph 7.10 and Graph 7.11 with Graph 7.12). This increase is due to an effective increase in the camber of the aerofoil as the flap is deflected downward. Due to an effective in the camber the flow separation is also increased. In the increment of flow separation the pressure drag is increased and also the skin frictions drag. Then the net drag is increased. So the drag co-efficient is increases with the flow angle of attack. In the above Graph 7.10  $C_D$  at  $-4^\circ$  is more than 0.05 and  $C_D$  at  $+15^\circ$  is 0.3. This result is high compare than blade without flap, blade with flap at  $5^\circ$  deflected, blade with flap at  $10^\circ$  deflected and blade with flap  $15^\circ$  deflected.

### 7.2.7. $C_D$ VS $\alpha$ FOR WITH FLAP AT DEFLECTED $25^\circ$ DOWNWARD DIRECTION

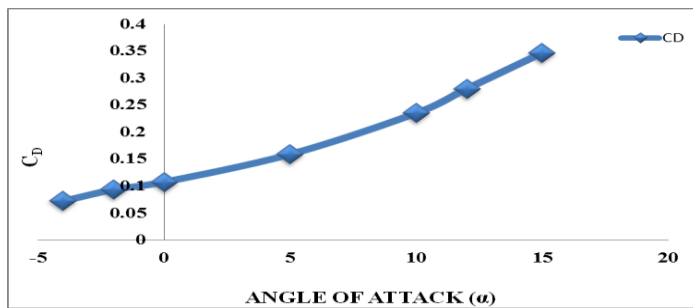


**Graph 7.13** ( $C_D$  VS  $\alpha$  FOR WITH FLAP AT DEFLECTED  $25^\circ$  DOWNWARD DIRECTION)

The above is the co-efficient of drag for different angle of attack for wind turbine blade with flap at deflected  $25^\circ$ . We can clearly understand the drag increased with increase of angle of attack. In the above Graph 7.13 the drag co-efficient

at angle of attack  $-2^\circ$  is suddenly deviated (decreased) from our expectation. It may be occurs due to the problem in meshing of the aerofoil or geometrical error or computational problem. In the above Graph 7.13  $C_D$  at  $-4^\circ$  is more than 0.06 and  $C_D$  at  $+15^\circ$  are more than 0.3. This result is high compare than blade without flap, blade with flap at  $5^\circ$  deflected, blade with flap at  $10^\circ$  deflected, blade with flap  $15^\circ$  deflected and blade with flap  $20^\circ$  deflected.

**7.2.7.  $C_D$  VS  $\alpha$  FOR WITH FLAP AT DEFLECTED  $30^\circ$  DOWNWARD DIRECTION**

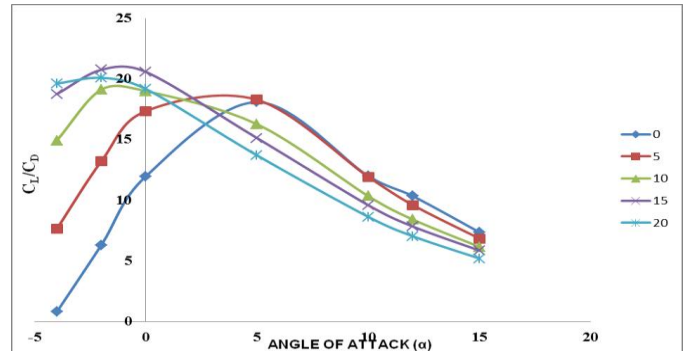


**Graph 7.14 ( $C_D$  VS  $\alpha$  FOR WITH FLAP AT DEFLECTED  $30^\circ$  DOWNWARD DIRECTION)**

The above is the co-efficient of drag for different angle of attack for wind turbine blade with flap at deflected  $30^\circ$ . We can clearly understand the drag increased with increase of angle of attack. A trailing edge flap is simply a portion of the trailing edge section of the aerofoil that is hinged and which can be deflected downward, as sketched in the insert in Graph 7.14. The positive angle  $30^\circ$  in Graph 7.14, the drag co-efficient is increased (compare the Graph 7.8, Graph 7.9, Graph 7.10, Graph 7.11, Graph 7.12 and Graph 7.13 with Graph 7.14). This increase is due to an effective increase in the camber of the aerofoil as the flap is deflected downward. Due to an effective in the camber the flow separation is also increased. In the increment of flow separation the pressure drag is increased and also the skin frictions drag. Then the net drag is increased. So the drag co-efficient is increases with the flow angle of attack. In the above Graph 7.14  $C_D$  at  $-4^\circ$  is more than 0.07 and  $C_D$  at  $+15^\circ$  is more than 0.34. This result is high compare than blade without flap, blade with flap at  $5^\circ$  deflected, blade with flap at  $10^\circ$  deflected, blade with flap  $15^\circ$  deflected, blade with flap  $20^\circ$  deflected and blade with flap  $25^\circ$  deflected

**7.3. LIFT TO DRAG RATIO FOR 2D MODELS**

An effective aerofoil produces lift with a minimum of drag; that is, the ratio of lift-to-drag is a measure of the aerodynamic efficiency of an aerofoil. The standard aerofoil have high lift-to-drag (L/D) ratio. And also the co-efficient of lift-to-drag ratio is increased with the angle of attack (AOA). The performance of wind turbine blade is directly proportional to the lift-to-drag ratio (L/D). The Graphs 7.1 to 7.7 show the variation of lift co-efficient versus angle of attack. We see  $C_L$  increasing linearly with angle of attack until a maximum value is obtained near  $15^\circ$ , beyond which there is a precipitous drop in lift. The  $C_L$  value varies from 0.1 to a maximum of 1.5509, covering a range of angle of attack from  $-4^\circ$  to  $15^\circ$ . Many aspects of the flight performance and also our wind turbine blade performance are directly related to the L/D ratio.

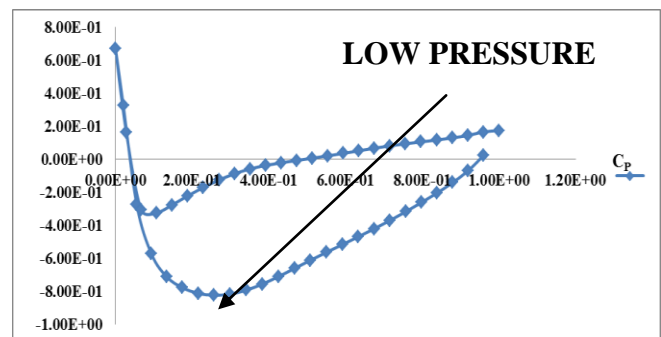


**Graph 7.15 (LIFT TO DRAG RATIO FOR 2D MODELS)**

The Graph 7.15 shows, for a different flap deflection angle. Then that at a given angle of attack, the deflection of flaps increases  $C_L$  value. On the other hand, the maximum L/D ratio is increased. Thus, the L/D ratio for a blade without high lifting device (flap) is much small to compare than the blade with high lifting device (flap). Due to the addition of flap in the trailing edge of the wind turbine blade the L/D ratio is increased, we can clearly understand these changes from Graph 7.15. In Graph 7.15 the L/D ratio is increased with increase angle of flap deflected.

**7.4. PRESSURE CO-EFFICIENT FOR 2D MODELS**

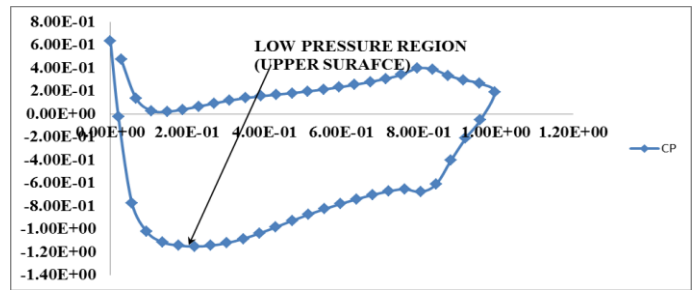
The pressure measurements were carried out for the complete experimental matrix described in an aerofoil section. The results from these measurements are discussed in this section. Typical pressure distribution curves and plots are presented. Graphs (7.16 to 7.22) shows the pressure coefficient curves for the upper and lower surface of the wing, plotted against the percent chord ( $x/c$ ) for  $Re=684740$  at  $\alpha=0^\circ$  with different flap deflection of the wind turbine blade. Graphs (7.23 to 7.25) presents the same plots for  $Re = 684740$  at  $\alpha = 5^\circ$  with different flap deflection of the wind turbine blade, Graphs (7.26 to 7.28) presents the same plots for  $Re = 684740$  at  $\alpha = 10^\circ$  with different flap deflection of the wind turbine blade, Graph 5.4 we can clearly understand the pressure distribution is high at the lower surface of an aerofoil and low at the upper surface of an aerofoil.



**Graph 7.16 ( $C_P$  VS  $X/C$  AT AOA  $0^\circ$  FOR WITHOUT FLAP)**

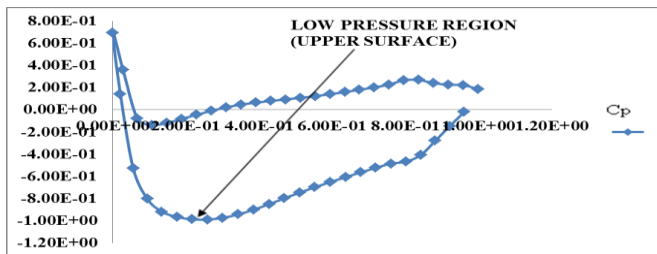
Graph 7.16 is plot  $C_P$  vs.  $X/C$  of the wind turbine blade without flap at  $0^\circ$  angle of attack. In the above graph the maximum pressure (stagnation pressure) occurs in the 0th position of  $X/C$  that means the stagnation pressure occurs on the leading edge of the wind turbine blade. In the upper the  $C_P$  is decrease dramatically to larger negative values. In the upper

surface the pressure is decreased from the stagnation point to higher negative values. In the low pressure region the pressure is very low in  $0.2 < X/C < 0.4$ , here the pressure value is -0.8. After that position 0.4 the pressure is typically increased in the low pressure region. This low pressure is disappeared at  $0.9 < X/C < 1.0$ . After that position it reaches the positive values. Similarly in the high pressure region the pressure is also decreased from the leading edge that means decrease from the stagnation point. In this lower surface the pressure is very low at  $0.1 < X/C < 0.2$ , here pressure value is near than -0.3. After that position  $X/C=0.2$  the pressure value is increased and it reach positive value at  $0.4 < X/C < 0.7$ . The maximum pressure is 0.2 in the position of  $1.0 < X/C < 1.1$ . Due to the low pressure in the upper surface the high pressure region from the lower surface is move to the upper surface. Due to this flow the lift is created. The area between the upper and lower surface  $C_p$  curves is a measure of the lift co-efficient. So the area between the upper and lower surface  $C_p$  curves is increased the lift co-efficient is also increases.



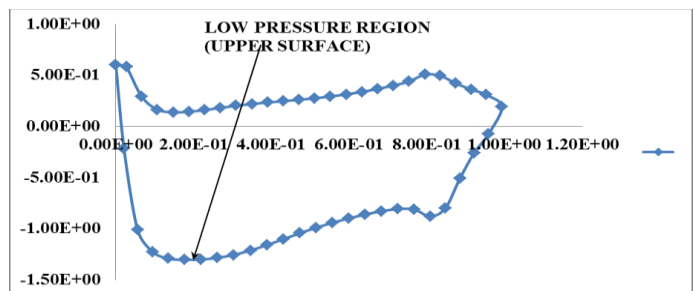
**Graph 7.18** ( $C_p$  VS  $X/C$  AT AOA  $0^\circ$  FOR FLAP DEFLECTED AT  $10^\circ$ )

Graph 7.18 is plot  $C_p$  vs.  $X/C$  of the wind turbine blade with flap deflected  $10^\circ$  at  $0^\circ$  angle of attack. In the above graph the maximum pressure (stagnation pressure) occurs in the 0th position of  $X/C$  that means the stagnation pressure occurs on the leading edge of the wind turbine blade. In the upper the  $C_p$  is decrease dramatically to larger negative values. In the upper surface the pressure is decreased from the stagnation point to higher negative values. In the low pressure region the pressure is very low in  $0.2 < X/C < 0.4$ , here the pressure value is -1.15. After that position 0.4 the pressure is typically increased in the low pressure region. This low pressure is disappeared at  $1.0 < X/C < 1.1$ . After that position it reaches the positive values. Similarly in the high pressure region the pressure is also decreased from the leading edge that means decrease from the stagnation point. In this lower surface the pressure is very low at  $0.1 < X/C < 0.2$ ; here pressure value is near than 0.148. After that position  $X/C=0.206$  the pressure value is increased at  $0.3 < X/C < 0.4$ . The maximum pressure is 0.1997 in the position of  $1.0 < X/C < 1.1$ . Similarly we plot the graph between  $C_p$  vs.  $X/C$  for wind turbine flap deflected at  $15^\circ$ ,  $20^\circ$ ,  $25^\circ$  and  $30^\circ$ . The Graphs for those cases are given below.

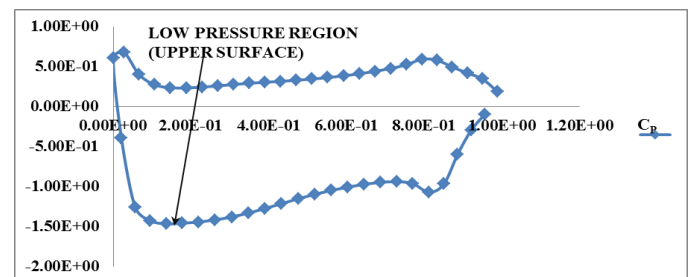


**Graph 7.17** ( $C_p$  VS  $X/C$  AT AOA  $0^\circ$  FOR FLAP DEFLECTED AT  $5^\circ$ )

Graph 7.17 is plot  $C_p$  vs.  $X/C$  of the wind turbine blade with flap deflected  $5^\circ$  at  $0^\circ$  angle of attack. In the above graph the maximum pressure (stagnation pressure) occurs in the 0th position of  $X/C$  that means the stagnation pressure occurs on the leading edge of the wind turbine blade. In the upper the  $C_p$  is decrease dramatically to larger negative values. In the upper surface the pressure is decreased from the stagnation point to higher negative values. In the low pressure region the pressure is very low in  $0.2 < X/C < 0.4$ , here the pressure value is -1.0. After that position 0.4 the pressure is typically increased in the low pressure region. This low pressure is disappeared at  $1.0 < X/C < 1.1$ . After that position it reaches the positive values. Similarly in the high pressure region the pressure is also decreased from the leading edge that means decrease from the stagnation point. In this lower surface the pressure is very low at  $0.1 < X/C < 0.2$ , here pressure value is near than -0.1. After that position  $X/C=0.2$  the pressure value is increased and it reach positive value at  $0.3 < X/C < 0.4$ . The maximum pressure is 0.2 in the position of  $1.0 < X/C < 1.1$ . In the Graph 7.17 the area between the lower & upper surface is high compare than the Graph 7.16, due to this reason the wind turbine blade with flap deflected 5o produced lift more than blade without flap.

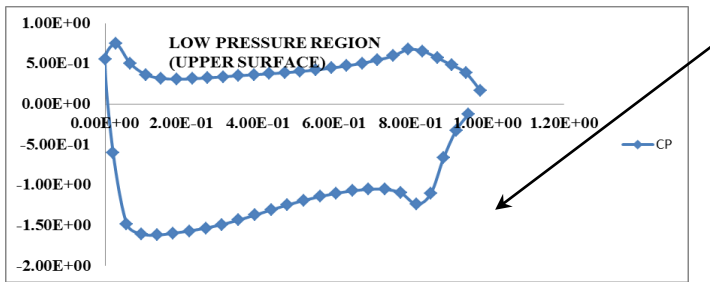


**Graph 7.19** ( $C_p$  VS  $X/C$  AT AOA  $0^\circ$  FOR FLAP DEFLECTED AT  $15^\circ$ )

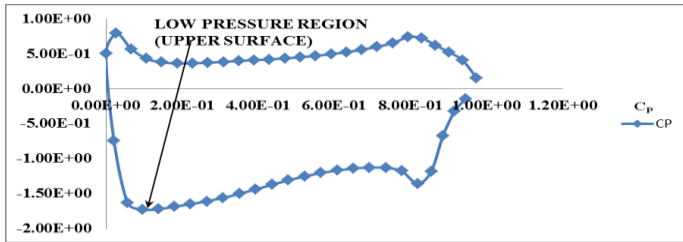


**Graph 7.20** ( $C_p$  VS  $X/C$  AT AOA  $0^\circ$  FOR FLAP DEFLECTED AT  $20^\circ$ )



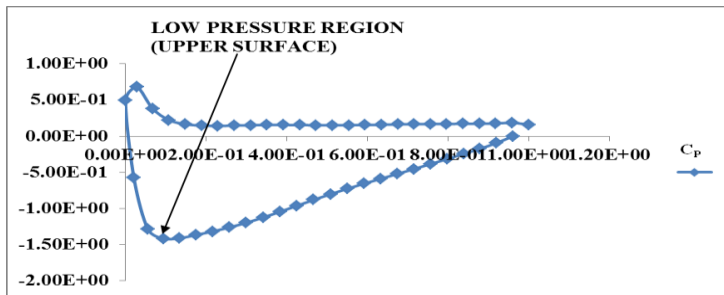


**Graph 7.21** ( $C_p$  VS  $X/C$  AT AOA  $0^\circ$  FOR FLAP DEFLECTED AT  $25^\circ$ )



**Graph 7.22** ( $C_p$  VS  $X/C$  AT AOA  $0^\circ$  FOR FLAP DEFLECTED AT  $30^\circ$ )

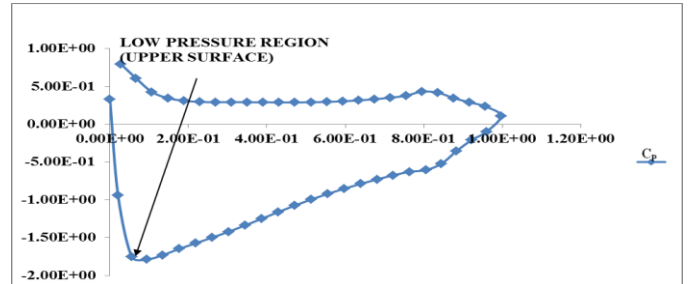
From the Graphs 7.16 to 7.22, we can clearly understand the area between the lower & upper surface of  $C_p$  curves is increased increase of flap deflection of wind turbine blade. Due to this the lift is increased with the increase of flap deflection of wind turbine blade. And also the area between the lower & upper surface of  $C_p$  curves of wind turbine blade with flap is more than wind turbine blade without flap.



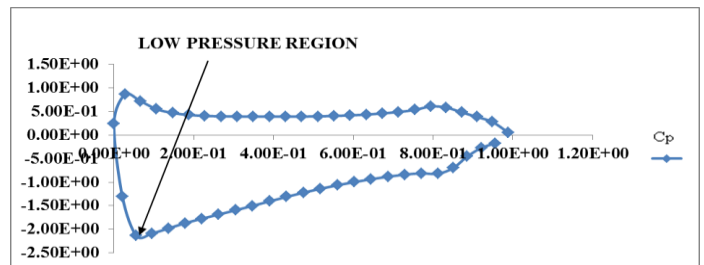
**Graph 7.23** ( $C_p$  VS  $X/C$  AT AOA  $5^\circ$  FOR FLAP DEFLECTED AT  $0^\circ$ )

Graph 7.23 is plot  $C_p$  vs.  $X/C$  of the wind turbine blade without flap at  $5^\circ$  angle of attack. In the above graph the maximum pressure (stagnation pressure) occurs in the 0th position of  $X/C$  that means the stagnation pressure occurs on the leading edge of the wind turbine blade. In the upper the  $C_p$  is decrease dramatically to larger negative values. In the upper surface the pressure is decreased from the stagnation point to higher negative values. In the low pressure region the pressure is very low in  $0.2 < X/C < 0.3$ , here the pressure value is  $-0.934$ . After that position  $0.3$  the pressure is typically increased in the low pressure region. This low pressure is disappeared at  $0.9 < X/C < 1.0$ . After that position it reaches the positive values. Similarly in the high pressure region the pressure is also decreased from the leading edge that means decrease from the stagnation point. In this lower surface the pressure is very low at  $1.0 = X/C$ , here pressure value is near

than  $0.17$ . Before this position  $X/C < 0.2$  the pressure value is high and here the pressure value is  $0.277$ . In this above Graph 7.23 in the lower surface the pressure is equal from the  $0.2^{nd}$  position to  $0.9^{th}$  position. Due to the low pressure in the upper surface the high pressure region from the lower surface is move to the upper surface. Due to this flow the lift is created. The area between the upper and lower surface  $C_p$  curves is a measure of the lift co-efficient. So the area between the upper and lower surface  $C_p$  curves is increased the lift co-efficient is also increases.

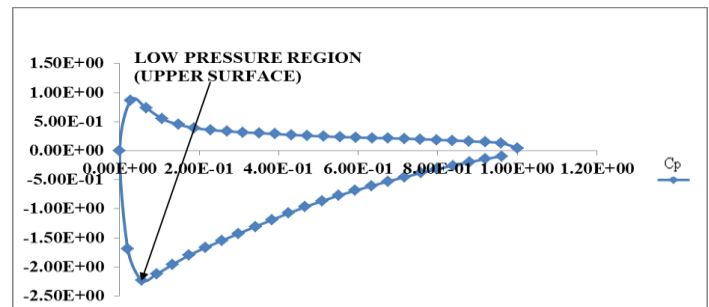


**Graph 7.24** ( $C_p$  VS  $X/C$  AT AOA  $5^\circ$  FOR FLAP DEFLECTED AT  $10^\circ$ )

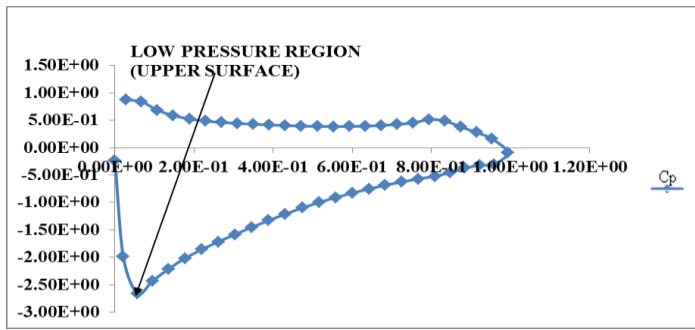


**Graph 7.25** ( $C_p$  VS  $X/C$  AT AOA  $5^\circ$  FOR FLAP DEFLECTED AT  $20^\circ$ )

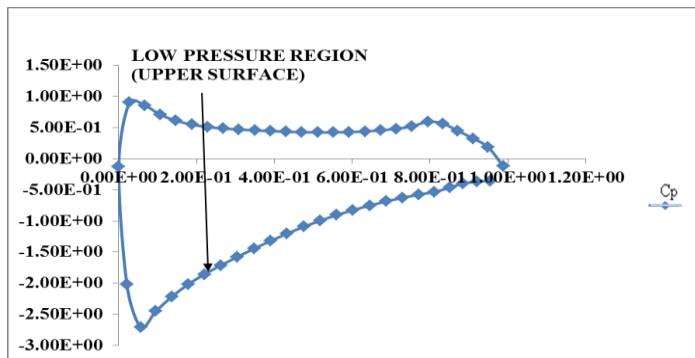
From the Graphs 7.23 to 7.25, we can clearly understand the area between the lower & upper surface of  $C_p$  curves is increased increase of flap deflection of wind turbine blade. Due to this the lift is increased with the increase of flap deflection of wind turbine blade. And also the area between the lower & upper surface of  $C_p$  curves of wind turbine blade with flap is more than wind turbine blade without flap.



**Graph 7.26** ( $C_p$  VS  $X/C$  AT AOA  $10^\circ$  FOR FLAP DEFLECTED AT  $0^\circ$ )



**Graph 7.27** ( $C_p$  VS  $X/C$  AT AOA  $10^\circ$  FOR FLAP DEFLECTED AT  $15^\circ$ )



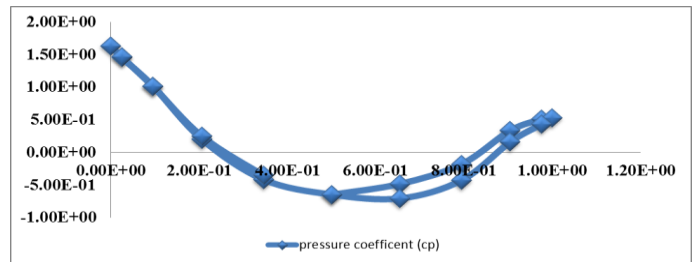
**Graph 7.28** ( $C_p$  VS  $X/C$  AT AOA  $10^\circ$  FOR FLAP DEFLECTED AT  $20^\circ$ )

From the above Graphs 7.16 to 7.28, we can clearly understand the area between the lower & upper surface of  $C_p$  curves is increased increase of flap deflection of wind turbine blade with different air angle of attack.

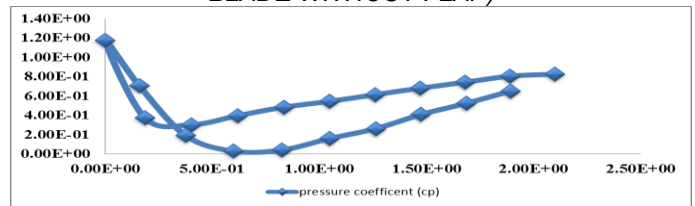
**7.5. PRESSURE CO-EFFICIENT FOR 3D MODELS**

In pervious in this chapter we discussed about pressure co-efficient for 2D models and now we goes to discuss about the pressure co-efficient for 3D models. And here we make an Iso-surface for different length like 3m, 4m, 5.5m, 20m, 32m and 40m and plot the  $C_p$  graph for that Iso-surface. If we did not make an Iso-surface and plot  $C_p$  means we cannot get the clear result that is why we make the Iso-surface and get a pressure distribution for particular area of the wind turbine blade. The below Graph7.29 is the pressure distribution for the cut section of the cylinder from the 3m of hub or rotor head of the wind turbine blade. In the above graph the maximum pressure (stagnation pressure) occurs in the 0th position of  $X/C$  that means the stagnation pressure occurs on the leading edge of the wind turbine blade. In the upper the  $C_p$  is decrease dramatically to larger negative values. In the upper surface the pressure is decreased from the stagnation point to higher negative values. In the low pressure region the pressure is very low in  $0.6 < X/C < 0.7$ , here the pressure value is  $-0.704$ . After that position 0.7 the pressure is typically increased in the low pressure region. This low pressure is disappeared at  $0.7 < X/C < 0.8$ . After that position it reaches the positive values. Similarly in the high pressure region the pressure is also decreased from the leading edge that means decrease from the stagnation point. In this lower surface the pressure is very low at  $0.6 < X/C < 0.7$ ; here pressure value is near than  $-0.647$ . After that position  $0.6 < X/C < 0.9$  the pressure

value is increased and it reaches positive value. The maximum pressure is 0.532 in the position of  $1.0 < X/C < 1.2$ .

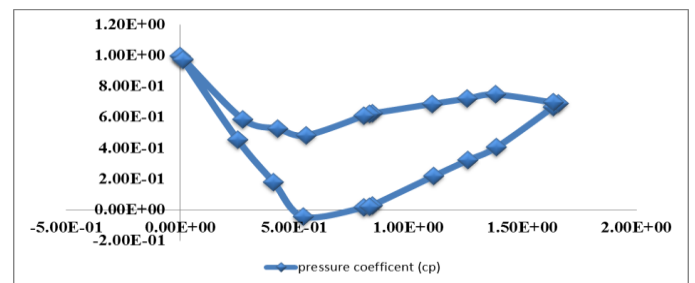


**Graph 7.29** ( $C_p$  VS  $X/C$  AT 3M FROM ROTOR HEAD IN BLADE WITHOUT FLAP)



**Graph 7.30** ( $C_p$  VS  $X/C$  AT 5.5M FROM ROTOR HEAD IN BLADE WITHOUT FLAP)

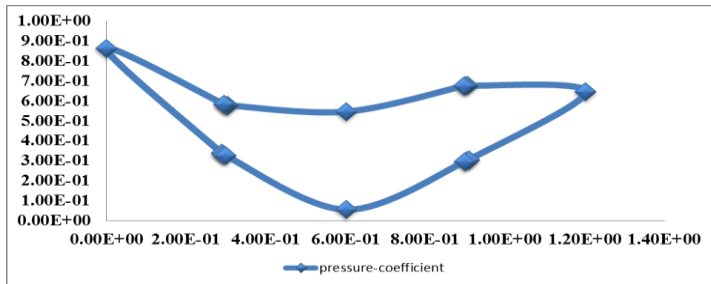
The above Graph7.30 is the pressure distribution for the cut section of the cut section from the 5.5m of hub or rotor head of the wind turbine blade. In the above graph the maximum pressure (stagnation pressure) occurs in the 0th position of  $X/C$  that means the stagnation pressure occurs on the leading edge of the wind turbine blade. In the upper surface the pressure is decreased from the stagnation point. In the low pressure region the pressure is very low in  $0.6 < X/C < 0.9$ , here the pressure value is 0.004. After that position 0.9 the pressure is typically increased in the low pressure region. Similarly in the high pressure region the pressure is also decreased from the leading edge that means decrease from the stagnation point. In this lower surface the pressure is low at  $0.4 < X/C < 0.5$ ; here pressure value is near than 0.3. After that position  $0.6 < X/C < 0.9$  the pressure value is increased. The maximum pressure is 0.8 in the position of  $2.1 < X/C < 2.2$ .



**Graph 7.31** ( $C_p$  VS  $X/C$  AT 20M FROM ROTOR HEAD IN BLADE WITHOUT FLAP)

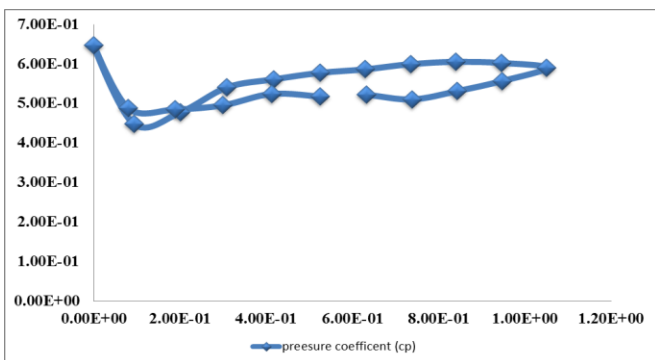
The above Graph7.31 is the pressure distribution for the cut section of the cut section from the 20m of hub or rotor head of the wind turbine blade. In the above graph the maximum pressure (stagnation pressure) occurs in the 0th position of  $X/C$  that means the stagnation pressure occurs on the leading edge of the wind turbine blade. In the upper the  $C_p$  is decrease dramatically to negative values. In the upper

surface the pressure is decreased from the stagnation point to negative values. In the low pressure region the pressure is very low in  $0.5 < X/C < 0.6$ , here the pressure value is -0.044. After that position 0.7 the pressure is typically increased in the low pressure region. This low pressure is disappeared at  $0.8 < X/C < 0.9$ . After that position it reaches the positive values. Similarly in the high pressure region the pressure is also decreased from the leading edge that means decrease from the stagnation point. In this lower surface the pressure is low at  $0.5 < X/C < 0.6$ ; here pressure value is near than 0.47. After that position  $0.6 < X/C < 0.7$  the pressure value is increased. The maximum pressure is 0.732 in the position of  $1.3 < X/C < 1.4$ . In this section the area between the upper and lower surface is high compare than other cut sections. In this cut section lift is high due to this reason moment is occurred and the blade will start rotate.



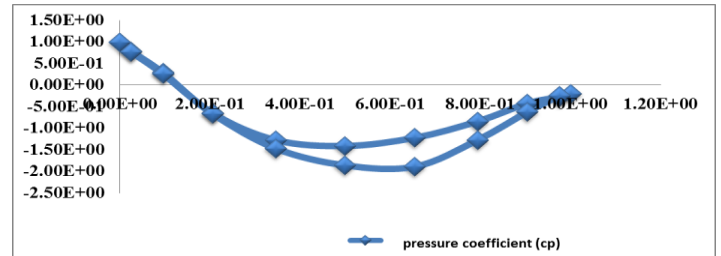
**Graph 7.32** ( $C_p$  VS  $X/C$  AT 35M FROM ROTOR HEAD IN BLADE WITHOUT FLAP)

The above Graph7.32 is the pressure distribution for the cut section of the cut section from the 35m of hub or rotor head of the wind turbine blade. In the above graph the maximum pressure (stagnation pressure) occurs in the 0th position of  $X/C$  that means the stagnation pressure occurs on the leading edge of the wind turbine blade. In the upper the  $C_p$  is decrease dramatically. In the upper surface the pressure. In the low pressure region the pressure is low in  $0.6 < X/C < 0.7$ , here the pressure value is 0.055. After that position 0.7 the pressure is typically increased in the low pressure region. Similarly in the high pressure region the pressure is also decreased from the leading edge that means decrease from the stagnation point. In this lower surface the pressure is low at  $0.3 < X/C < 0.6$ ; here pressure value is near than 0.57. After that position  $0.6 < X/C < 0.7$  the pressure value is increased. The maximum pressure is 0.676 in the position of  $0.9 < X/C < 1.0$ .



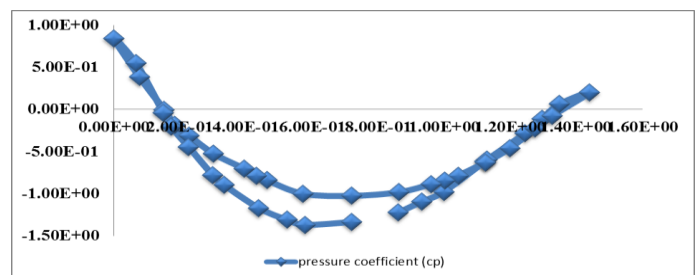
**Graph 7.33** ( $C_p$  VS  $X/C$  AT TIP OF THE WND TURBINE BLADE WITHOUT FLAP)

The above Graph7.33 is the pressure distribution for the tip of the wind turbine blade. In the above graph the maximum pressure (stagnation pressure) occurs in the 0th position of  $X/C$  that means the stagnation pressure occurs on the leading edge of the wind turbine blade. In the upper and the lower surface the  $C_p$  is decrease dramatically. Here the area between the upper and lower surface is very low at the tip of the wind turbine blade.



**Graph 7.34** ( $C_p$  VS  $X/C$  AT 3M FROM ROTOR HEAD IN BLADE WITH FLAP DEFLECTED AT  $20^\circ$ )

The above Graph 7.34 is the pressure distribution for the cut section of the cylinder from the 3m of hub or rotor head of the wind turbine blade. In the above graph the maximum pressure (stagnation pressure) occurs in the 0th position of  $X/C$  that means the stagnation pressure occurs on the leading edge of the wind turbine blade. In the upper the  $C_p$  is decrease dramatically to larger negative values. In the upper surface the pressure is decreased from the stagnation point to higher negative values. In the low pressure region the pressure is very low in  $0.5 < X/C < 0.7$ , here the pressure value is -1.89. After that position 0.4 the pressure is typically increased in the low pressure region. Similarly in the high pressure region the pressure is also decreased from the leading edge that means decrease from the stagnation point. In this lower surface the pressure is very low at  $0.4 < X/C < 0.5$ ; here pressure value is near than -1.41.

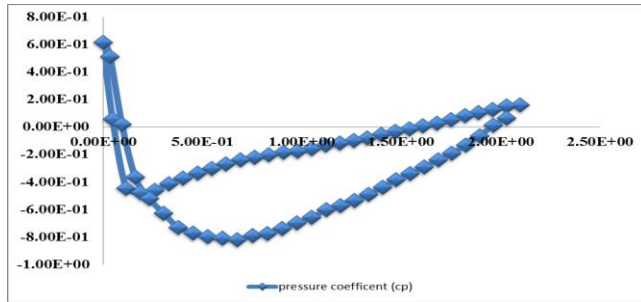


**Graph 7.35** ( $C_p$  VS  $X/C$  AT 4M FROM ROTOR HEAD IN BLADE WITH FLAP DEFLECTED AT  $20^\circ$ )

The above Graph 7.35 is the pressure distribution for the cut section of 4m from the hub or rotor head of the wind turbine blade. In the above graph the maximum pressure (stagnation pressure) occurs in the 0th position of  $X/C$  that means the stagnation pressure occurs on the leading edge of the wind turbine blade. In the upper the  $C_p$  is decrease dramatically to larger negative values. In the upper surface the pressure is decreased from the stagnation point to higher negative values. In the low pressure region the pressure is very low in  $0.5 < X/C < 0.6$ , here the pressure value is -1.37. After that position 0.8 the pressure is typically increased in the low

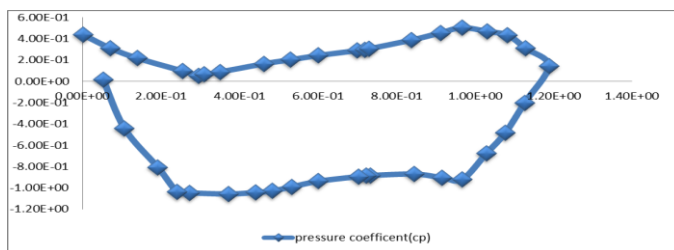


pressure region. This low pressure is disappeared at  $1.2 < X/C < 1.4$ . After that position it reaches the positive values. Similarly in the high pressure region the pressure is also decreased from the leading edge that means decrease from the stagnation point. In this lower surface the pressure is very low at  $0.7 < X/C < 0.8$ ; here pressure value is near than  $-1.03$ . After that position  $1.2 < X/C < 1.4$  the pressure value is increased and it reaches positive value. The maximum pressure is  $2.01$  in the position of  $1.4 < X/C < 1.5$ .



**Graph 7.36** ( $C_p$  VS  $X/C$  AT 5.5M FROM ROTOR HEAD IN BLADE WITH FLAP DEFLECTED AT  $20^\circ$ )

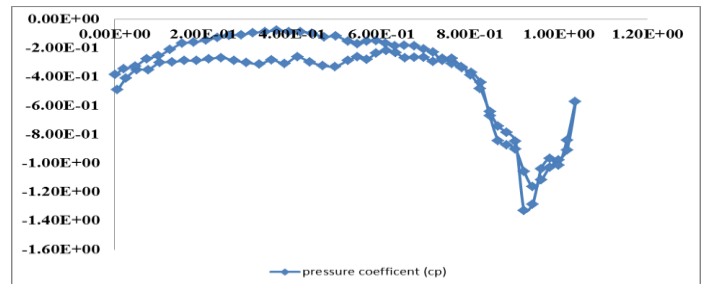
The above Graph 7.36 is the pressure distribution for the cut section of 5.5m from the hub or rotor head of the wind turbine blade. In the above graph the maximum pressure (stagnation pressure) occurs in the 0th position of  $X/C$  that means the stagnation pressure occurs on the leading edge of the wind turbine blade. In the upper the  $C_p$  is decrease dramatically to larger negative values. In the upper surface the pressure is decreased from the stagnation point to higher negative values. In the low pressure region the pressure is very low in  $0.6 < X/C < 0.7$ , here the pressure value is  $-0.8$ . After that position  $0.7$  the pressure is typically increased in the low pressure region. This low pressure is disappeared at  $1.8 < X/C < 2$ . After that position it reaches the positive values. Similarly in the high pressure region the pressure is also decreased from the leading edge that means decrease from the stagnation point. In this lower surface the pressure is very low at  $0.18 < X/C < 0.2$ ; here pressure value is near than  $-0.47$ . After that position  $1.5 < X/C < 1.6$  the pressure value is increased and it reaches positive value. The maximum pressure is  $0.19$  in the position of  $2.0 < X/C < 2.2$ .



**Graph 7.37** ( $C_p$  VS  $X/C$  AT 35M FROM ROTOR HEAD IN BLADE WITH FLAP DEFLECTED AT  $20^\circ$ )

The above Graph 7.37 is the pressure distribution for the cut section of 35m from the hub or rotor head of the wind turbine blade. In the above graph the maximum pressure (stagnation pressure) occurs in the 0th position of  $X/C$  that means the stagnation pressure occurs on the leading edge of the wind turbine blade. In the upper the  $C_p$  is decrease dramatically to

larger negative values. In the upper surface the pressure is decreased from the stagnation point to higher negative values. In the low pressure region the pressure is very low in  $0.3 < X/C < 0.4$ , here the pressure value is  $-1.05$ . After that position  $0.9$  the pressure is typically increased in the low pressure region. This low pressure is disappeared at  $1.1 < X/C < 1.2$ . After that position it reaches the positive values. Similarly in the high pressure region the pressure is also decreased from the leading edge that means decrease from the stagnation point. In this lower surface the pressure is very low at  $0.2 < X/C < 0.3$ ; here pressure value is near than  $0.05$ . After that position  $0.2 < X/C < 0.3$  the pressure value is increased. The maximum pressure is  $0.5$  in the position of  $0.9 < X/C < 1$ .



**Graph 7.38** ( $C_p$  VS  $X/C$  AT THE TIP OF THE WIND TURBINE BLADE WITH FLAP DEFLECTED AT  $20^\circ$ )

The above graph 7.38 is the pressure distribution of the tip of the wind turbine blade. Here the pressure is too low compare then other cut section of the blade.

## 8. CONCLUSION

In this project we analysis the flow around the wind turbine blade (with and without flap). And we compare the results of co-efficient of pressure, lift co-efficient and lift to drag ratio of blade with flap and without flap in different angle of flap deflection in 2D. In 3D we compare the co-efficient of pressure of wind turbine blade with and without flap in different cut section from rotor head or hub (3m, 4m, 5.5m, 20m, 35m & 40m) in different angle of flap deflection. In this project we analysis only for +ve direction (downward) deflection. Because in the upward deflection did not get an effective result. We got an effective result in downward deflection of flap in wind turbine blade especially  $20^\circ$  deflection of flap in wind turbine. More than  $20^\circ$  deflection of flap in wind turbine the lift drop occurs due to the increase of drag. By adding of flap in wind turbine we can increase the power production. Normally the wind turbine starts rotate at the 5m/s of wind speed but in the adding of flap in wind turbine blade the it will start rotate at 3.2m/s to 3.5m/s of wind speed. Due to that the efficiency of wind turbine will be increased. The airfoil configuration is selected as NACA 4415 for the blade configuration. Three bladed rotor models with 120 degree angle are considered. The diameter of the rotor is 90m, the blade length is 40m and height of the tower is 100m considered for the turbine configuration. The blade model will be modeled and meshed for the design analysis and the analysis will be done.

## 9. REFERENCES

- [1] Arturo baron and maurizio quadrio, turbulent boundary layer over riblets. conditional analysis of Ejection-like events, *int. J. Heat and fluid flow* 18:188-196, 1997
- [2] A. Baron and m. Quadrio, influence of riblets on the structure of a turbulent boundary layer, *int. J. Heat and fluid flow*, vol. 14, no. 3, september 1993
- [3] A. Baron, m. Quadrio and I. Vigevano, on the boundary layer/riblets interaction mechanisms and the prediction of turbulent drag reduction, *int. J. heat and fluid flow*, vol. 14, no. 4, december 1993
- [4] A. Pollard, passive and active control of near-wall Turbulence, *progress in aerospace sciences* vol. 33, pp. 689-708, 1997
- [5] J. Reneaux, overview on drag reduction technologies for civil transport aircraft, *europaean congress on computational methods in applied sciences and engineering Eccomas 2004*
- [6] K. N. Liu,\* c. Christodoulout, o. Ricciust, and d. D. Joseph, drag reduction in pipes lined with riblets, *aiaa journal* october 1990, vol. 28, no. 10
- [7] Michael'j. Walsh, riblets as a viscous drag reduction technique, *nasa langley research center, hampton, virginia*
- [8] O.a. El-samni , h.h. Chun , h.s. Yoon , drag reduction of turbulent flow over thin rectangular riblets, *international journal of engineering science* 45 (2007) 436–454
- [9] P.r. Viswanath, aircraft viscous drag reduction using riblets, *progress in aerospace sciences* 38 (2002) 571–600
- [10] S.-j. Lee, y.-g. Jang, control of flow around a naca 0012 airfoil with a micro-riblet film, *journal of fluids and structures* 20 (2005) 659–672
- [11] Zhang de-yuan, lu yue-hao, li xiang, chen hua-wei, numerical simulation and experimental study of dragreducing Surface of a real shark skin, *science direct-journal of hydrodynamics*